Title

Exploration of the carmaphycins as payloads in antibody drug conjugate anticancer agents

Authors

Almaliti, Jehad
Miller, Bailey
Pietraszkiewicz, Halina
et al.

Publication Date

2019

DOI

10.1016/j.ejmech.2018.10.024

Peer reviewed

HHS Public Access

Author manuscript

Eur J Med Chem. Author manuscript; available in PMC 2020 January 01.

Published in final edited form as:

Eur J Med Chem. 2019 January 01; 161: 416–432. doi:10.1016/j.ejmech.2018.10.024.

Exploration of the Carmaphycins as Payloads in Antibody Drug Conjugate Anticancer Agents

Jehad Almaliti[a,b], **Bailey Miller**[a], **Halina Pietraszkiewicz**[e], **Evgenia Glukhov**[b], **C. Benjamin Naman**[a,f], **Toni Kline**[d], **Jeffrey Hanson**[d], **Xiaofan Li**[d], **Sihong Zhou**[d], **Frederick A. Valeriote**[e], and **William H. Gerwick**[a,c,*]

[a]Center for Marine Biotechnology and Biomedicine, Scripps Institution of Oceanography, University of California San Diego, La Jolla, California 92093, United States

[b]Department Pharmaceutical Sciences, College of Pharmacy, the University of Jordan, Amman, 11942, Jordan

[c]Skaggs School of Pharmacy and Pharmaceutical Sciences, University of California San Diego, La Jolla, California 92093, United States

[d]Sutro Biopharma, South San Francisco, California 94080 United States

[e]Department of Internal Medicine, Division of Hematology and Oncology, Henry Ford Hospital, Detroit, MI 48202, USA

[f]College of Food and Pharmaceutical Sciences, Ningbo University, Ningbo, Zhejiang, 315211, China

Abstract

Antibody–drug conjugates (ADCs) represent a new dimension of anticancer chemotherapeutics, with warheads to date generally involving either antitubulin or DNA-directed agents to achieve low- to sub-nanomolar potency. However, other potent cytotoxins working by different pharmacological mechanisms are under investigation, such as α,β-epoxyketone based proteasome inhibitors. These proteasome active agents are an emerging class of anticancer drug that possesses ultra-potent cytotoxicity to some cancer cell lines. The carmaphycins are representatives of this latter class that we isolated and characterized from a marine cyanobacterium, and these as well as several synthetic analogs exhibit this level of potency. In the current work, we investigated the use of these highly potent cytotoxic compounds as warheads in the design of novel ADCs. We designed and synthesized a library of carmaphycin B analogues that contain amine handles, enabling their attachment to an antibody linker. The basicity of these incorporated amine handles was shown to strongly affect their cytotoxic properties. Linear amines resulted in the greatest reduction in cytotoxicity whereas less basic aromatic amines retained potent activity as

*Author for correspondences: telephone 858-534-0578; wgerwick@ucsd.edu.

Supplementary data

Supplementary data related to this article can be found at: http://dx.doi.org/

demonstrated by a 4-sulfonylaniline derivative. These investigations resulted in identifying the P2 residue in the carmaphycins as the most suitable site for linker attachment point, and hence, we synthesized a highly potent analog of carmaphycin B that contained a 4-sulfonylaniline handle as an attachment point for the linker antibody.

Graphical Abstract

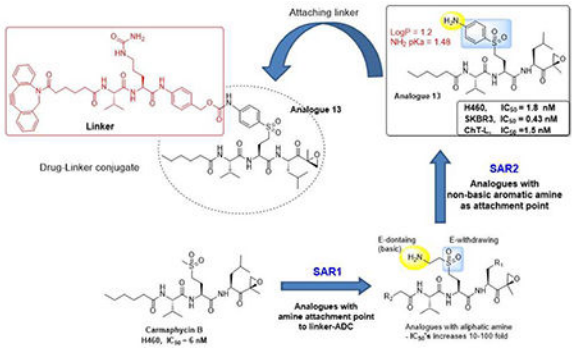

Keywords

Anticancer drugs; proteasome inhibitors; antibody-drug conjugate; amine basicity optimization; 4-sulfonylaniline; carmaphycins

Introduction

Antibody-drug conjugates (ADCs) have become an established class of targeted agents in the treatment of neoplastic diseases.[1,2] ADCs consist of an antibody linked to a highly potent cytotoxic agent that selectively targets a specific antigen overexpressed on tumor cells. This results in the combination of a potent cytotoxic warhead with the selectivity of an antibody to enable targeted cell killing. The antibody guides the conjugate to the targeted site of action and, following internalization into lysosomes, the cytotoxin is released leading to cell death (Figure 1). Four FDA approved ADCs are currently in clinical use, MYLOTARG® (gemtuzumab ozogamicin), ADCETRIS® (brentuximab vedotin), BESPONSA® (inotuzumab ozogamicin) and KADCYLA® (ado-trastuzumab emtansine).[3] In addition, more than 50 additional ADCs are in various stages of clinical trial.[3] The vast majority of the clinical trial agents, as well as two of the currently approved ADCs, utilize anti-mitotic compounds, such as auristatin and maytansine derivatives, as the cytotoxic warhead. While these agents have proven successful, there is great interest to explore warhead cytotoxins that operate via different mechanisms of action.[1,3–5]

Filamentous marine cyanobacteria have emerged as a key source of novel lead compounds for drug discovery and development, especially in the area of new anticancer therapeutics.[6,7] The majority of their metabolites emanate from hybrid biosynthetic pathways that involve both polyketide synthases (PKSs) and non-ribosomal peptide synthetases (NRPSs), and hence are nitrogen rich.[6,8] Due to their specific interactions with various cellular targets, several marine cyanobacterial compounds are under investigation for their utility in a

number of disease areas, including neurodegenerative disorders, inflammation, infectious diseases and cancer.[9]

Recently, we isolated and characterized carmaphycins A (**1**) and B (**2**) from a Curaçao collection of the marine cyanobacterium *Symploca sp.*, and they displayed potent activity against a number of cancer cell lines (Figure 2).[10] Subsequently, they were found to inhibit the β5 subunit (chymotrypsin-like activity) of the proteasome at low nanomolar concentrations.[10,11] The inhibitory properties of carmaphycins A and B were subsequently evaluated against the *Saccharomyces cerevisiae* 20S proteasome and found to possess IC_{50} values of 2.5 nM and 2.6 nM, respectively, comparable to those reported for epoxomicin (**3**) and the marine-derived salinosporamide A (**4**) IC_{50} of 2.7 nM and 1.4 nM, respectively).[10]

The carmaphycins are structurally related to the known proteasome inhibitor epoxomicin (Figure 2),[10] and feature a leucine-derived terminal α,β-epoxyketone warhead attached to a methionine sulfoxide in **1** or methionine sulfone in **2**. Carfilzomib (**5**), a proteasome inhibitor based on epoxomicin and possessing the α,β-epoxyketone warhead, was FDA approved in 2012 for the treatment of multiple myeloma.[12] A number of other α,β-epoxyketone based proteasome inhibitors are being investigated for their anticancer utility as stand-alone agents, such as ixazomib citrate,[13] oprozomib[14] and delanzomib.[15,16] Inhibition of the proteasome, a proteolytic complex responsible for the degradation of ubiquitinated proteins, has emerged as a powerful strategy in the treatment of cancer.[17,18] However, because of their high potency, selectivity of action is less than desired, and toxic side effects are common. We therefore hypothesized that utilizing a highly toxic carmaphycin derivative as the warhead of an ADC might provide the required potency and achieve a better selectivity profile.

Results

2.1. Design and cytotoxicity evaluation of carmaphycin B analogues

Structurally, the carmaphycins can be divided into four distinct sections (P1-P4); the first features an α,β-epoxyketone pharmacophore (the P1 residue) followed by the unique methionine sulfoxide in **1** or methionine sulfone in **2** (the P2 residue). This is in turn is connected to a valine moiety (the P3 residue) and completed with a hexanoate chain as the terminus (the P4 residue, Figure 3). In our previously published docking and crystallization studies of carmaphycin B with the chymotrypsin-like (ChT-L) site of the yeast 20S proteasome,[10,11] we observed the P1 leucine side chain was in close proximity to methionine, alanine and valine residues in the hydrophobic S1 pocket. On the other hand, the side chain of the P2 methionine sulfone residue extended out of the binding pocket and likely interacts with external solvent molecules. The P3 valine side chain was found to interact with a hydrophobic cluster of three alanine residues in the S3 pocket. Finally, the P4 hexanoate tail was observed to interact with another hydrophobic cluster consisting of Pro104, Tyr106, Pro127, and Val128.[10,11]

We had two main goals in the current study. First, we aimed to refine structure-activity relationships in the carmaphycin structure class so as to produce more potent analogues, and

second, we sought to introduce an amine functional group as a handle for attaching the molecule through a linker to an antibody while retaining high cytotoxic potency. To achieve these goals, we designed analogues with modifications at P1-P4 both with and without the amine handle. Herein we describe the design, synthesis and biological evaluation of these carmaphycin analogues as potential new payloads for an ADC, and identify the 4-sulfonylaniline as a relatively non-basic moiety for attachment to the antibody linker.

The designed analogues all incorporated sulfone methionine derivatives at the P2 position (similar to carmaphycin B) rather than the sulfoxide methionine as in carmaphycin A, as this eliminated structural complexity arising from the mixture of stereoisomers at the sulfoxide group. An amine functional group was introduced in each derivative so as to produce an attachment point to the linker and antibody.

Initially, we synthesized a first generation analogue possessing an amine group at the distal terminus of P4; the hexanoate chain was replaced with 6-amino hexanoate (analogue **6**, Figure 4). However, introducing this P4 substitution reduced cytotoxicity considerably to NCI-H460 cells compared to the parent compound [**6**, IC_{50} = 860 nM; carmaphycin B (**2**), IC_{50} = 6 nM]. This reduction in cytotoxic potency was mirrored by a significant reduction in binding affinity to the ChT-L site of the proteasome [**6**, IC_{50} = 539 nM; carmaphycin B (**2**), IC_{50} = 2.6±0.9 nM].[10] Analysis of the X-ray structure for the yeast 20S proteasome in complex with carmaphycin A revealed that P4 makes a significant contact with a lipophilic S4 surface pocket (Figures 3 and 4). Hence, this was concluded to be a poor site for introduction of a polar moiety for linkage to the antibody section of the drug complex.

Alternatively, since the P2 side chain extends outwards of the peptide binding pocket and is therefore solvent exposed, it was predicted to better tolerate the presence of polar residues such as a primary amino group. In addition, Mroczkiewicz e*t al* have demonstrated that the constitutive proteasome P2 pocket is the only pocket that can tolerate major changes and have shown that it can accommodate a non-natural amino acid stereoisomer, as demonstrated by the potent activity of the analogue MG-132 with a D-amino acid at P2.[19] Consequently, the second generation carmaphycin analogues were designed to contain an amine handle on the P2 side chain (Figure 5). Five compounds (analogues **7–11**) were initially designed which contained a 2aminoethyl homocysteine residue at P2 instead of the methionine sulfone present in carmaphycin B. To improve hydrophobic interactions of the P1, P3 and P4 side chains with their respective S1, S3 and S4 binding pockets, the linear alkyl chains were replaced with aromatic phenyl or pyridine rings. Investigations with other proteasome inhibitors, such as carfilzomib and its analogs, have shown that introducing bulky hydrophobic groups at P3 and P4 increase binding affinity.[20,21] The pyridine analogue **11** was designed to evaluate whether a combination of hydrophobic interaction plus presence of a hydrogen bonding acceptor at P1 might be advantageous.[20]

Initial evaluation of compounds **7–11** was performed on HCT116 colon adenocarcinoma and NCI-H460 human lung cancer cell lines. Two trends emerged from these evaluations. First, it became clear that incorporating an ethyl amine terminus at the P2 position clearly resulted in a significant reduction of cytotoxic potency in both cancer cell lines compared to the lead compound, carmaphycin B. This reduction in cytotoxicity was more prominent in HCT116

cells with a 3–15 fold difference in IC_{50} values (Table 1). We reasoned that this loss of cytotoxic activity might be due to a reduction in binding affinity of the analogues to the ChT-L site of the proteasome. Alternatively, because the aliphatic amine at P2 is basic and thus positively charged at physiological pH, the decreased potency could simply reflect reduced cell permeability. Therefore, we also evaluated the tert-butoxycarbonyl (Boc)-protected derivatives (**7**-Boc – **11**-Boc, Figure 5 and Table 1) for their cytotoxic activity in both cell lines. These hydrophobic capped analogs possessed similar potencies to the parent structures (all in the low nM range), supporting the hypothesis that it was the charged nature of **7–11** that was responsible for this reduced potency.

To further confirm this proposal, compound **7** as well as its Boc-protected precursor **7**-Boc were evaluated for proteasome inhibitory activity at the ChT-L site. Purified 26S proteasomes from rabbit muscle were used in assays employing site-specific fluorogenic substrates. The two compounds possessed very similar inhibitory activities against the ChT-L site with IC_{50} values of 2.5 and 8.1 nM, respectively (Table 3), comparable to that of carmaphycin B (IC_{50} = 22.5 nM). This series of experiments thus confirmed that the reduced potency of the free ethylamine analogs **7–11** was due to cell impermeability caused by the positively charged basic amine at physiological pH, and thus was not considered a problem in the design of an ADC which would be taken up into cells by the mechanism depicted in Figure 1. However, we also considered that the charged nature of these analogs at lysosomal pH might impact their release from the lysosome, and thus we investigated alternative functionalities as described below.

Secondly, replacing the P1 leucine residue with phenylalanine generally resulted in a loss of potency. For example, analogue **10** with a P1 phenylalanine-derived α,β-epoxyketone, a P3 phenylalanine residue and a P4 phenyl-acetic acid residue, was significantly less potent in both cell lines than corresponding analogue **8** with a P1 leucine-derived terminal α,β-epoxyketone. However, interaction of different residues in determining potency was revealed with analogues **7** and **9** in that they were somewhat more potent in NCI-H460 cells despite a P1 Phe residue, presumably as a result of smaller non-aromatic residues at P3 and P4. Replacing P1 with a pyridyl-alanine side chain in **11**-Boc led to further loss of potency.

Accordingly, to reduce the basicity of the free amine at P2, an analogue was designed that incorporates an electron withdrawing sulfone moiety (Figure 6). The P2 methyl sulfone portion of carmaphycin B was substituted with a 4-thioaniline in **12** or the oxidized 4-sulfonylaniline in **13** to generate less basic analogues. The theoretical pKa of the 4-sulfonylaniline in analogue **13** is about 2.5, while that of the 4-thioaniline **12** is 5–6 and the ethyl amine in analogues **7–11** is 910. This reduction in pKa predicted that analogues **12** and **13** would not be protonated at physiological pH, and hence they should retain their favorable membrane permeability properties. In contrast to what was observed in the alkyl amines above (**7–11**), analogues **12**-Boc and **13**-Boc were somewhat less active than their deprotected counterparts **12** and **13** (Table 1). In addition, the 4-sulfonylaniline analogue **13** was more potent than the 4-thioaniline analogue **12**, supporting the hypothesis that the less basic amine would have increased potency due to its lower hydrophilicity and resulting better cell and membrane permeability. Analogue **13** was also the more potent inhibitor at both the ChT-L (IC_{50} 1.1 nM) and the trypsin-like (T-L) sites (IC_{50} 14 nM)(Table 3).

To explore additional chemical handles for the antibody linkage as well as to eliminate the undesirable effects of the basic amine on potency and cell permeability, we synthesized a set of analogues containing two leucyl-epoxyketone pharmacophores at both P1 and P2 (figure 7). In analogue **14** the methionine sulfone of carmaphycin B was replaced with glutamic acid that was coupled to a second leucyl-epoxyketone, yielding the double electrophile analogue **14**. Biological evaluation of analogue **14** (Table 1) showed exceptionally potent activity against the HCT116 cell line (IC_{50} 0.2 nM) and low nanomolar IC_{50} against the NCI-H460 cell line (IC_{50} 5.4 nM).

Inspired by the remarkable potency of analogue **14** to the HCT116 cell line, two analogues were produced (**15**, **16**) with aniline moieties at either P3 or P4 to provide a weakly basic amine handle for antibody-drug linkage (Figure 7). In addition, to investigate if the potent activity of analogue **14** was due to a better fit of the epoxyketone in the active site when placed at the P2 site, we designed analogue **17** that contains the same glutamic acid–leucine-EK at P2 whereas methionine-4-sulfo-aniline replaced the leucine-EK at P1 (Figure 7). This latter modification allowed us to explore P1 as a potentially new conjugation site. The three analogues **15–17** were evaluated against three different cancer cell lines, HCT116, MDA-MB-468 and SKBR3, and the results are summarized in Table 2. Unfortunately, analogue **17** as well as its Boc-protected intermediate **17**-Boc had almost no effect on these cell lines (IC_{50}'s in the micromolar range). Replacing the P1 epoxyketone with a 4-sulfonyl-aniline-modified methionine residue also resulted in significant reduction in activity, demonstrating that the epoxyketone warhead at P1 is essential for the potent cytotoxic activity in analogue **14**. Thus, it appears that the second epoxyketone at P2 in **14** may improve activity through a better fit at P2, and is not necessarily directly involved in the covalent inhibition of the enzyme. Analogue **15** (Table 2) with its P3 aniline-containing side chain showed reduced cytotoxicity compared to the **14**; it was most potent to SKBR3 cells (IC_{50} = 21 nM). Interestingly, the Boc-protected precursor **15**-Boc was somewhat less active against the same cell lines (Table 2), indicating that the S3 binding pocket can tolerate relatively basic residues, but that bulky groups like Boc are less well accommodated at this position.

Interestingly, placing an aniline functionality at the P4 position in analogue **16** resulted in a more potent cell growth inhibitor compared to analogue **15** (Table 2). Furthermore, in contrast to what was observed in analogue **15** and **15**-Boc, intermediate **16**-Boc was 4–5 fold more potent as a cell growth inhibitor than the free amine **16**. Analogue **16** possessed double digit nM IC_{50}'s in the three cell lines whereas Boc-protected **16** was consistently active with single digit nM IC_{50}'s (Table 2). This result supports out previous finding for analogue **6**, namely that the S4 pocket does not accommodate highly basic residues. This is reflected in the rank order potencies of the lipophilic Boc-protected **16**, the moderately basic aniline **16** and the highly basic alkyl amine **6**. Moreover, this observation is consistent with our previous X-ray crystallography study of carmaphycin B, which revealed that the P4 binding pocket (S4) is large and hydrophobic.[11]

We also investigated the impact of replacing the methionine sulfone at P2 with methyl glutamine (**19**) or dimethyl glutamine (**20**) on cytotoxic activity (Figure 7). In NCI-H460 cell lines, both analogs **19** and **20** possessed comparable potency to carmaphycin B,

suggesting that the glutamine amide group functions as hydrogen bond acceptor similar to the sulfone (Table 2). To further investigate this latter point, the P2 hydrogen bond acceptor was eliminated in analogue **18** and reduced in **21** by replacing the methionine sulfone with a methylene or sulfide group, respectively. The inhibitory activity of analogue **21** was largely retained, possibly due to the hydrogen bond forming capability of sulfides,[10] whereas that of **18** was significantly reduced, indicating the importance of this hydrogen bonding feature. A similar trend was observed for the cytotoxic activity of analogues **18–21** against the HCT116 cell line (Table 2). It should also be noted that the P2 sulfide derivative **21** represents what we believe is the actual natural product produced by the cyanobacterium, and that this becomes non-enzymatically oxidized to the racemic methionine sulfoxide (**1**, carmaphycin A) and then the sulfone (**2**, carmaphycin B) upon extraction and isolation. In fact, using MS^2-based molecular networking,[22] we were able to identify a peak with a mass consistent with the P2-methionine residue in a related cyanobacterium collected from Panama (see Supporting Information, Figure S1).

2.2. Inhibitory effects on the human 20S proteasome

Epoxyketone-based inhibitors generally possess potent activity to the chymotrypsin-like (ChTL_ site of the proteasome and are less potent against the trypsin-like (T-L) and caspase-like (CL) sites.[23] Indeed, the ChT-L site is the primary target of the approved anticancer agents bortezomib and carfilzomib; however, inhibitors of the T-L site are known to sensitize cancer cells to these agents.[20,24] To understand the growth inhibitory properties of these carmaphycin analogs, we evaluated the inhibitory activity of several analogues (**7**, **7**-Boc, **13**, **15**, **15**-Boc, **16**, **16**-Boc, **17**, **22** and **23**) at the three active sites of the proteasome. These were evaluated using the fluorogenic substrates Suc-LLVY-AMC, Cbz-LLE-AMC, and Cbz-VGR-AMC, respectively, and the results are summarized in Table 3. While the major focus of our designed agents targeted potency at the ChT-L site, some of these analogues were found to possess rather remarkable potency at the T-L site.

The rationale for testing the P2 alkyl amines **7** and **7**-Boc at the ChT-L site was to understand if the loss of activity of **7** was due to lower binding affinity or decreased cell permeability. The ChT-L site IC_{50} values of these two analogues were closely similar (**7**-Boc, IC_{50} = 14.2 ± 2.4 nM; **7**, IC_{50} = 22.2 ± 5.4nM) indicating that they have similar binding affinities to the ChT-L site; therefore, the decreased cellular potency of analogue **7** is most likely due to reduced cell permeability, similar to analog **6**. Next, the high cytotoxic potency of analogue **13** in the NCIH460 cell line inspired its evaluation to all three active sites in the proteasome. It was found exquisitely potent to the ChT-L site (IC_{50} = 1.5 ± 0.24 nM), relatively potent to the T-L site (IC_{50} = 14 nM) and weakly active to the C-L site (IC_{50} = 540 nM). The superior potency of **13** at all three sites relative to carmaphycin B suggests that the *P*-sulfo-aniline moiety is more favorably accommodated than a methionine sulfone at the P2 position. Similarly, analogue **14** showed inhibitory activity to the three proteasome catalytic sites similar to that of analogue **13**, and was especially potent to the chymotrypsin-like site (ChT-L IC_{50} =1.9 ± 0.11 nM); analogue **13** was also potently cytotoxic to cells.

We also evaluated the proteasome inhibitory activities of the three double warhead analogues **15–17** that were designed based on compound **14** (Table 3). The weak cytotoxic

activity of analogue **17** wherein the epoxyketone and sulfonylaniline moieties were exchanged between P1 and P2 was consistent with the observed lack of inhibitory activity at all three proteasome sites (IC_{50}'s >1000 nM). Surprisingly, analogue **15** and its **15**-Boc derivative were more potent inhibitors at the ChT-L site compared to analogue **16** and **16**-Boc, a finding that was inconsistent with the several fold increased cytotoxic potency of **16** over **16**-Boc. However, both analogues **16** and **16**-Boc were about 3-fold more potent against the T-L site compared to **15** and **15**-Boc, and this might be contributing to the potency of these analogues (Table 3). A recent study published by Geurink and coworkers showed that inhibition of the T-L site can sensitize cancer cells to cytotoxic chemotherapeutics.[20]

2.3. Chemistry

Generalized synthesis of carmaphycin analogues—The generalized route for the synthesis of the epoxyketone moiety in the carmaphycins is illustrated in Scheme 1. Commercially available Boc-protected amino acid derivatives (e.g. **25**) were converted into the corresponding Weinreb amides (e.g. **26**), followed by treatment with Grignard reagent, isopropenylmagnesium bromide, to yield conjugated enones (e.g. **27**). Luche reduction (sodium borohydride and cerium (III) chloride) was used to convert the enones into the corresponding alcohols (e.g. **28**; 2S, 3R). The allylic alcohol was treated with *t*butylhydroperoxide in the presence of vanadyl acetylacetonate as catalyst to obtain epoxides (e.g. **29**), which were converted directly to the epoxyketones (e.g. **30**) using Dess-Martin periodinane oxidation.[10,20]

The P2 moiety of analogues **7–11**, which contains a terminal amine modified methionine residue for conjugation, were synthesized as outlined in Scheme 2.[29] The synthesis of the *S*-alkylated homocysteine building block **37** began with the esterification of L-homocystine **31** to provide dimethyl ester **32**; this was reacted with Fmoc-Cl and potassium carbonate to yield the fully protected homocystine **33**. Reduction of the disulfide bond was achieved with zinc powder in trifluoroacetic acid/methanol (TFA/MeOH) under an argon atmosphere to yield Fmoc-homocysteine methylester **34**. The sulfur was then alkylated with 2-(Boc-amino)ethyl bromide in the presence of cesium carbonate to afford sulfide **35**. Oxidation of sulfide **35** with mCBPA yielded sulfone **36**. Removal of the Fmoc protecting group using diethylamine afforded the crude amine **37** which was partially purified on SiO_2 and then used in subsequent steps.

The construction of analogues **7–11** is shown in scheme 3, which was achieved by coupling the amino acids at P2 to those of P3 and then acylation of the amino terminus with the appropriate alkyl group at P4 for each analogue.[20] In brief, homocysteine derivative **37** was coupled to Boc-L-Val or Boc-L-Phe using standard HBTU/HOBt coupling. The Fmoc-protected peptide was deprotected using diethylamine and acylated with hexanoic acid or phenyl acetic acid to obtain the acylated dipeptide (e.g. **40**), which was hydrolyzed to the carboxylic acid using lithium hydroxide. This was followed by HBTU/HOBt coupling of the appropriate epoxyketone moiety **30** to obtain the final analogues **7**-Boc to **11**-Boc. These analogues were deprotected using TFA/DCM and purified on deactivated silica gel to obtain the free amine of analogues **7–11**. Construction of these analogues in the opposite sense,

namely beginning at the *N*-terminus and coupling amino acids onto the *C*-terminus, led to racemization of the corresponding alpha centers and thus was not pursued further.[10]

Finally, the P2-*para*-sulfonylaniline analogues **12** and **13** were prepared according to scheme 4. Commercially available L-homoserine was brominated using HBr and acetic acid to obtain L-2-amino-4-bromobutanoic acid **41**. This was esterified using thionyl chloride and protected with Fmoc-Cl to provide fully protected compound **42**.[30] Di-*tert*-butyl dicarbonate was used to convert 4-aminobenzenethiol **43** to *tert*-butyl-*N*-(4-sulfanyphenyl)carbamate **44**, which was used to alkylate bromo compound **42** to afford the sulfide **45**. The Fmoc group in **45** was removed using diethylamine and the product was coupled with Fmoc-L-Val to give **47**. The Fmoc in **47** was removed and the product acylated with hexanoic acid. Subsequently, the sulfide was oxidized using mCBPA to afford sulfone **48**. The methyl ester in **48** was hydrolyzed and the product coupled with the Leu-epoxyketone moiety to give analogues **12**-Boc and **13**-Boc. The two Boc protected derivatives were deprotected using standard conditions and purified over triethylamine-deactivated silica gel to afford analogues **12** and **13**.

2.4. Preparation of drug-linker precursors for analogues 7-Boc and 13, their bioconjugation to the antibody trastuzumab and biological evaluation of the ADC.

Based on the structure-activity relationships described above, as well as the X-ray structure of carmaphycin B bound in the yeast 20S proteasome active site,[11] the P2 side chain was identified as the most suitable position for introducing an amine group as the linkage position to an antibody. Because analogues **13** and **7**-Boc displayed potent activity against both the NCIH460 cell line and the ChT-L site of the proteasome, these two analogues were chosen for modification with a linker for antibody conjugation. Analogue **7**-Boc demonstrated potent cytotoxicity only in the Boc-protected form, and therefore we selected a “non-cleavable” linker for analogue **7** to create compound **22** as the payload for antibody conjugation. In contrast, because analogue **13** was highly potent as the free amine, we selected a protease-cleavable linker for this compound to generate compound **23**.[25]

Synthesis of the non-cleavable linker was straightforward: commercially available DBCO-C6acid was acylated onto compound **7** to obtain derivative **22** (Figure 8). Compound **23** was generated from the DBCO-C6-acid coupled to valine (V), citrulline (C) and 4-aminobenzyloxycarbonyl (PABC) as the traditional carbamate (Figure 8). In either case, the linkers in compounds **22** and **23** contained a terminal alkyne moiety as part of the dibenzylcyclooctyne (DBCO) group. This was reacted with azide-containing antibodies using strain promoted alkyne azide cycloaddition (SPAAC) to generate the complete ADC. The purpose of the C6 dicarboxylic acid in both derivatives was to provide a spacer; this was deemed especially important for compound **23** to provide enough room for the valine-citrulline section to be recognized and cleaved at the adjacent citrulline-PABC amide bond by cathepsin B. Once this bond is cleaved, the remaining linker section spontaneously decomposes to release 4aminobenzyl alcohol, CO_2 and the free cytotoxic drug **13**.

Compound **22** was assembled in high yield by a simple HATU/HOAt coupling reaction between the aliphatic amine in **7** and the DBCO-C6 acid (Figure 9). However, synthesis of

the cleavable linker drug conjugate **23** was more challenging. This first involved formation of the carbamate between Fmoc-valine-citrulline-PAB alcohol with the amine of **13** to give intermediate **24**, followed by Fmoc deprotection and coupling with the DBCO-C6 acid to yield **23** (Figure 10). We anticipated that the aromatic amine of analogue **13** would be weakly nucleophilic because of the strongly electron withdrawing *para*-sulfone group; this was borne out by our experimental results. Initial attempts at forming carbamate **24** by reacting **13** with triphosgene to generate the isocyanate intermediate and quenching by addition of Fmoc-VC-PAB alcohol, only resulted in traces of product **24** (1–2% yields). The use of various other solvents (DMF, EtOAc, THF and dioxane) or bases ($NaHCO_3$, DIPEA and NEt_3) did not improve the yield. Reacting Fmoc-VCPAB-OH with triphosgene first and then quenching the intermediate with amine **13** also proved unsuccessful. Replacing the triphosgene with carbonyldiimidazole (CDI) did not yield any carbamate product **24**; however, modifying the initial route by using phosgene rather than triphosgene to generate the isocyanate led to moderate success. Following optimization of this route using different solvents and reaction temperatures (Table 4 and Figure 10), the best yields were realized when the alcohol Fmoc-VC-PAB-OH was dissolved in acetonitrile and added to the isocyanate intermediate, followed by overnight reflux in a sealed tube (yield 23%). The Fmoc-protected product **24** was then deprotected using Hunig's base followed by coupling with the DBCO-C6-acid using HBTU and HOBt to obtain compound **23** (Figure 10). It is noteworthy that evaporating the deprotected intermediate of **24** to complete dryness led to significant degradation as a result of intramolecular reaction of the transiently formed free amine with the epoxyketone moiety.

Site-specific conjugation to the antibody via incorporation of an orthogonally reactive amino acid has been demonstrated to confer significant advantages to ADCs, and cell free protein synthesis enables this strategy.[26] Conjugates of compounds **22** and **23** with trastuzumab were prepared as described in the literature,[27] and their cytotoxic proprieties were evaluated against three adherent cancer cell lines [SKBR3 (Her2 +) and MDA-MB-468 (Her 2 -) and MDA-MB231 (Her 2 -)]. Additionally, we also tested the free analogues **7**-Boc and **13** as well as the corresponding drug-linker complexes **22** and **23**.[28] Cell killing results for Her2-positive (SKBR3) and -negative (MDA-MB-468) cells are shown in Figure 11 and Table 5. Analogues **7**Boc and **13** show high potency against the three cell lines with compound **13** being the most active; sub-nanomolar IC_{50} to SKBR3 and MDA-MB-231. The cytotoxic activity of **13** was of about 6-fold less than that of MMAE. The drug-linker complex **23** was of reduced potency compared to the corresponding free warhead **13**, a result perhaps expected because of the bulky nature of the linker. However, there was no enhanced cell killing by the antibody-drug conjugates (ADCs) of either **13** or **7** in the susceptible Her2-positive SKBR3 cells compared to the free antibody trastuzumab. In most cases, the IC_{50} curves of these carmaphycin ADC complexes showed reduced efficacy compared to that of the **MMAE** ADC, an unexpected result given the high potency of the free compound **13** against SKBR3 cells. We speculate that this may result from either protein-mediated degradation of the carmaphycin backbone once conjugated, lysosomal degradation of the carmaphycin derivative, or inappropriate ADC trafficking. However, this lower potency may also be a direct reflection of the 6 to 100 fold intrinsic potency differences between MMAE and **7-Boc** and **13**.

Conclusions

The carmaphycins are a new marine-derived class of epoxy-ketone proteasome inhibitor, some of which possess exquisite potency suitable for use as warheads in ADC-type antitumor drugs. Initial efforts revealed the critical requirement for a lipophilic tail in these agents so as to retain high potency to the proteasome as well as to cells, and thus conjugation to a linker and antibody through a terminal amine functionality was ineffective. High basicity of an ethyl amine functionality at P2, a site generally solvent accessible, was shown to negatively alter membrane permeability, and hence this was also avoided as it may impede escape from the lysosome into the cell cytoplasm. Thus, we attenuated the basicity of this P2 amine-linkage position by introducing a sulfonylaniline moiety, and this provided potent cytotoxic analogues of carmaphycin B suitable for conjugation as novel ADC warheads. Although the free analogues retained high cytotoxic potency, the ADCs did not show superior cell killing against the tested cancer cell lines compared to the free antibody. However, this lower potency may also be a direct reflection of the 6- to 100-fold intrinsic potency differences between MMAE and **7-Boc** or **13**. Nonetheless, through these investigations to engineer the carmaphycin scaffold as an ADC payload, we have developed *inter alia* potent novel analogs and discovered some additional underlying SAR principles for this structure class. These, along with the understanding developed from our initial ADC results, can be applied to the design of a next generation of carmaphycin analogs as either stand-alone drug agents or as the warhead of an ADC.

EXPERIMENTAL SECTION

4.1. Material and Instrumentation:

All chemicals and solvents were purchased from commercial suppliers and used without further purification, unless stated otherwise. Anhydrous THF and ether were freshly distilled from sodium and benzophenone before use. A Jasco P-2000 polarimeter 314 was used to measure optical rotations. NMR spectra were recorded on a Varian 500 MHz spectrometer (500 and 125 MHz for the ^{1}H and ^{13}C nuclei, respectively) using $CDCl_3$, CD_3OD or CD_3CN as solvents from Cambridge Isotope Laboratories, Inc. Spectra were referenced to residual $CDCl_3$, CD_3OD or CD_3CN solvent as internal standard (for $CDCl_3$ δH 7.26 and δC 77.1; for CD_3OD δH 4.78 and δC 49.2; and for CD_3CN δH 1.93 and δC 1.3). LC-HRMS data for analysis of compounds **7**−**21** were obtained on an Agilent 6239 HR-ESI-TOFMS equipped with a Phenomenex Luna 5 μm C18 100 Å column (4.6 × 250 mm). LCMS data for purity analysis of the synthesized compounds **7**−**21** were obtained with a Thermo Finnigan Surveyor Autosampler-Plus/LC-Pump-Plus/PDA-Plus system and a Thermo Finnigan LCQ Advantage Max mass spectrometer (monitoring 200−600 nm and *m/z* 150−2000 in positive ion mode) using a linear gradient of 10 100% H_2O/acetonitrile over 15 – 20 min; flow rate of 1 mL/min. Semipreparative HPLC purification was carried out using a Waters 515 with a Waters 996 photodiode array detector using Empower Pro software. Structural integrity and purity of the test compounds were determined by the composite of ^{1}H and ^{13}C NMR, HRMS and HPLC, and all compounds were found to be >92% pure.

4.2. Synthetic Procedures:

General procedure for the synthesis of epoxy-ketone moiety (30a-c)—To a solution of Boc-protected amino acid (1 equiv), NH(Me)OMe·HCl (1.5 equiv) and HBTU (1.5 equiv) in DCM (0.28 M) was added DiPEA (4.5 equiv.) and the mixture was stirred at room temperature for 2 h until TLC showed completion of reaction. The solvent was evaporated under reduced pressure and the residue was resuspended in ethyl acetate. The organic layer was washed with 1M HCl (3×), saturated $NaHCO_3$ (2×), brine, and then dried using anhydrous sodium sulfate. It was evaporated under reduced pressure and the crude product was purified by column chromatography (25–75% ethyl acetate/hexanes) to give the Weinreb amides **26a-c** in quantitative yield as colorless oils.

To a solution of Weinreb amides **26** (1 equiv.) in THF (0.34 M) at 0 ^oC was added isopropenyl magnesium bromide solution (2.0 equiv., 0.5 M solution in THF) drop wise and the reaction was stirred at 0 ^oC overnight. After TLC indicated completion of the reaction, ice-cold saturated aqueous NH_4Cl solution was added followed by ethyl acetate. The organic layer were separated, extracted with brine, dried over anhydrous sodium sulfate and evaporated. The crude product was purified on column chromatography (25–75% ethyl acetate-hexanes) and the product was obtained as a colorless oil (yields 60–90%).

To a solution of enone **27** (1 equiv.) in methanol (0.17 M) at 0 °C was added $CeCl_3·7H_2O$ (1.5 eq.) and $NaBH_4$ (1.4 eq., 6.0 mmol, 227 mg) portion wise. The mixture was stirred for 25 minutes after which glacial acetic acid was added and the mixture was concentrated under reduced pressure. The resulting crude mixture was re-dissolved in ethyl acetate and extracted with saturated aqueous sodium bicarbonate, brine, dried over anhydrous sodium sulfate and concentrated in vacuo. Compound **28** was obtained as a yellow oil (quantitative yield) and used for the next step without further purification.

To a solution of allylic alcohol **28** (1 equiv.) in DCM (0.16 M) at 0 °C was added vanadyl acetylacetonate (0.1 eq.) and *t*-butyl hydroperoxide (3 eq.). The reaction mixture was stirred at same temperature for 2 h, and then was concentrated under reduced pressure, redissolved in ethyl acetate, extracted with saturated $NaHCO_3$, H_2O and brine, dried over sodium sulfate and concentrated under reduced pressure. The crude product was passed though a plug of silica (20–50% ethyl acetate/hexanes) and immediately subjected to the next step. The semi-pure compound was dissolved in DCM and Dess-Martin periodinane (1.5 eq.) was added. The mixture was stirred at room temperature overnight after which TLC analysis indicated complete conversion. The reaction was worked-up by addition of a $NaHCO_3$ (sat. aq.)/ $Na_2S_2O_3$ (1 M aq.) solution present in a 1:4 ratio and the resulting emulsion was stirred vigorously for 30 min. The layers were separated and the aqueous layer extracted with DCM. The combined organic layers were extracted with saturated $NaHCO_3$, dried over anhydrous sodium sulfate and concentrated under reduced pressure. The crude product was purified on column chromatography (10–50% ethyl acetate/hexanes) to yield the product as colorless oil (yield: 60–80% over 2 steps).

tert-butyl ((S)-4-methyl-1-((R)-2-methyloxiran-2-yl)-1-oxopentan-2-yl)carbamate (30a): $[\alpha]_D^{22}$ + 62.1 (*c* 0.7, $CHCl_3$). ^1H NMR (500 MHz, $CDCl_3$) δ 4.85 (d, *J* = 8.9 Hz, 1H), 4.41 – 4.26 (m, 1H), 3.30 (d, *J* = 5.0 Hz, 1H), 2.90 (d, *J* = 5.0 Hz, 1H), 1.81 – 1.68 (m,

1H), 1.60 – 1.57 (m, 1H), 1.53 (s, 3H), 1.42 (s, 12H), 1.18 (ddd, *J* = 14.2, 10.4, 4.1 Hz, 1H), 0.98 (d, *J* = 6.5 Hz, 4H), 0.94 (d, *J* = 6.7 Hz, 4H). ^{13}C NMR (125 MHz, $CDCl_3$) δ 209.7, 155.8, 79.9, 59.2, 52.5, 51.5, 40.6, 28.5, 25.3, 23.6, 21.5, 17.0. **HRMS**: (ESI) calcd for $C_{14}H_{25}NO_4$ $[M + H]^+$ 272.1861; found 272.1863.

tert-butyl ((S)-1-((R)-2-methyloxiran-2-yl)-1-oxo-3-phenylpropan-2-yl)carbamate (30b): $[\alpha]_D^{22}$ + 25.0 (*c* 0.2, $CHCl_3$). ^{1}H NMR (500 MHz, $CDCl_3$) δ 7.31 (d, *J* = 8.3 Hz, 2H), 7.28 – 7.23 (m, 1H), 7.17 (d, *J* = 7.5 Hz, 2H), 4.95 (d, *J* = 8.3 Hz, 1H), 4.59 (td, *J* = 8.0, 5.1 Hz, 1H), 3.29 (d, *J* = 4.9 Hz, 1H), 3.11 (dd, *J* = 13.9, 5.0 Hz, 1H), 2.91 (d, *J* = 4.9 Hz, 1H), 2.74 (dd, *J* = 14.0, 7.8 Hz, 1H), 1.51 (s, 3H), 1.37 (s, 12H). ^{13}C NMR (125 MHz, $CDCl_3$) δ 208.6, 155.4, 136.1, 129.6, 128.7, 127.2, 80.0, 59.4, 53.8, 52.6, 37.7, 28.4, 16.8. **HRMS**: (ESI) calcd for $C_{17}H_{23}NO_4$ $[M + H]^+$ 306.1705; found 306.1709.

tert-butyl ((S)-1-((R)-2-methyloxiran-2-yl)-1-oxo-3-(pyridin-4-yl)propan-2-yl)carbamate (30c): $[\alpha]_D^{22}$ + 29.2 (*c* 0.3, $CHCl_3$). ^{1}H NMR (500 MHz, $CDCl_3$) δ 8.58 – 8.44 (m, 2H), 7.12 (d, *J* = 5.0 Hz, 2H), 5.01 (d, *J* = 8.7 Hz, 1H), 4.61 (td, *J* = 8.5, 4.6 Hz, 1H), 3.28 (d, *J* = 4.8 Hz, 1H), 3.13 (dd, *J* = 13.9, 4.6 Hz, 1H), 2.95 (d, *J* = 4.8 Hz, 1H), 2.66 (dd, *J* = 13.9, 8.4 Hz, 1H), 1.53 (s, 3H), 1.36 (s, 12H). ^{13}C NMR (125 MHz, $CDCl_3$) δ 207.8, 155.3, 150.0, 145.4, 124.8, 80.4, 59.2, 53.1, 52.7, 37.2, 28.4, 16.7. **HRMS**: (ESI) calcd for $C_{16}H_{22}N_2O_4$ $[M + H]^+$ 307.1658; found 307.1667.

L-Homocystine bis-methyl ester (32)—To a suspension of **L**-homocystine (2.0 g, 7.50 mmol) in methanol (95 mL) was carefully added thionyl chloride (1.1 mL, 30.1 mmol) drop wise over 30 min. The reaction was stirred under nitrogen overnight, and then it was concentrated under reduced pressure to provide a yellow solid (2.78 g, quantitative yield). ^{1}H NMR (500 MHz, CD_3OD) δ 4.21 (s, 2H), 3.86 (s, 3H), 3.33 (m, 1H), 2.90 (m, 2H), 2.36 (d, *J* = 27.4 Hz, 2H). ^{13}C NMR (125 MHz, CD_3OD) δ 169.3, 53.1, 51.7, 51.7, 32.8, 29.9. **HRMS**: (ESI) calcd for $C_{10}H_{20}N_2O_4S_2$ $[M + H]^+$ 297.0943; found 297.0949.

Methyl *N*-(((9H-fluoren-9-yl)methoxy)carbonyl)-S-(2-((tert-butoxycarbonyl)amino)ethyl)- L-homocysteinate (35)—To **L**-homocystine bis-methyl ester (1.11 g, 3.75 mmol) in a round bottom flask was added a solution of potassium carbonate (3.11 g, 22.5 mmol, 6 equiv.) in H_2O (45 mL), followed by a dioxane solution (15 mL) of Fmoc-Cl (1.94 g, 7.5 mmol, 2 equiv.). The reaction was stirred vigorously for 3 h at which time a white precipitate formed; this was broken up by sonication and stirred for another 12 h. The reaction was sonicated one additional time and the white precipitate was filtered off and washed with methanol, dried and evaporated to afford the product as white solid (1.95 g, 70% yield). The product was used in the next step without further purification.

To a solution of bis-Fmoc-**L**-homocystine bis-methyl ester (0.56 g, 0.75 mmol) in methanol (35 mL) and dichloromethane (10 mL) was added TFA (2.31 mL, 30 mmol) and zinc dust (0.15 g, 2.25 mmol). The cloudy reaction mixture became clear after stirring overnight under nitrogen, at which time the zinc was removed by filtration. The filtrate was evaporated under reduced pressure and the residue redissolved in ethyl acetate and washed with 1M HCl, 1N NaOH and brine. The organic layer was dried over anhydrous sodium sulfate and

concentrated under reduced pressure to yield the crude product (0.51 g, 92% yield); this was taken to the next step without further purification.

To a solution of Fmoc-**L**-Homocysteine methyl ester **34** (0.155 g, 0.434 mmol) and N-Boc-bromoethylamine (0.146 g, 0.651 mmol, 1.5 equiv.) in DMF (5 mL) was added Cs_2CO_3 (0.17 g, 0.412 mmol, 1.2 equiv.) and the reaction was stirred under a nitrogen atmosphere overnight. The mixture was diluted in ethyl acetate (30 mL) and washed with 1 M HCl, $NaHCO_3$, brine and dried over anhydrous sodium sulfate. The crude product was purified on silica chromatography (20–70% ethyl acetate/hexanes) and the title product **35** was obtained as a colorless oil (0.107 g, 48% yield). $[\alpha]_D^{22}$ + 25.6 (*c* 0.4, $CHCl_3$). ^{1}H NMR (500 MHz, $CDCl_3$) δ 7.77 (d, *J* = 7.6 Hz, 2H), 7.61 (dd, *J* = 7.5, 4.7 Hz, 2H), 7.41 (t, *J* = 7.5 Hz, 2H), 7.32 (tt, *J* = 7.4, 1.2 Hz, 2H), 5.60 (d, *J* = 8.3 Hz, 1H), 4.97 (m, 1H), 4.51 (td, *J* = 8.0, 4.7 Hz, 1H), 4.46 – 4.37 (m, 2H), 4.23 (t, *J* = 6.9 Hz, 1H), 3.77 (s, 3H), 3.37 – 3.21 (m, 2H), 2.64 (t, *J* = 6.6 Hz, 2H), 2.61 – 2.52 (m, 2H), 2.20 – 2.10 (m, 1H), 1.97 (dq, *J* = 14.6, 7.4 Hz, 1H), 1.45 (s, 10H). ^{13}C NMR (125 MHz, $CDCl_3$) δ 172.6, 156.2, 156.0, 143.9, 141.5, 127.9, 127.3, 125.3, 120.2, 79.7, 67.2, 53.2, 52.8, 47.3, 39.7, 32.5, 32.3, 28.6, 27.6. **HRMS**: (ESI) calcd for $C_{27}H_{34}N_2O_6S$ $[M + H]^+$ 515.2216; found 515.2228.

Methyl (*S*)-2-((((9H-fluoren-9-yl)methoxy)carbonyl)amino)-4-((2-((tertbutoxycarbonyl)amino)ethyl)sulfonyl)butanoate (36)—To a solution of sulfide **35** (30 mg, 58.4 μmol) in dichloromethane was added *m*-CBPA (20 mg, 116.8 μmol) at 0 °C and the reaction was stirred at the same temperature for 30 min. The reaction was monitored by TLC and additional m-CBPA was added as necessary. The reaction was allowed to warm to room temperature, stirred overnight and then diluted with aqueous $NaHSO_3$ and partitioned between H_2O and ethyl acetate. The organic layer was washed with saturated $NaHCO_3$, brine, dried over anhydrous sodium sulfate then evaporated under reduced pressure. The crude product was purified on column chromatography (20–100% ethyl acetate/hexanes) to yield the sulfone **36** as white solid (28 mg, yield 78.8). m.p. 212–215 °C, $[\alpha]_D^{22}$ – 18.2 (*c* 0.5, $CHCl_3$). ^{1}H NMR (500 MHz, $CDCl_3$) δ 7.76 (d, *J* = 7.6 Hz, 2H), 7.58 (d, *J* = 7.5 Hz, 2H), 7.40 (t, *J* = 7.5 Hz, 2H), 7.35 – 7.29 (m, 2H), 5.60 (d, *J* = 8.1 Hz, 1H), 5.16 (s, 1H), 4.45 (dd, *J* = 13.2, 6.4 Hz, 3H), 4.21 (t, *J* = 6.7 Hz, 1H), 3.77 (s, 3H), 3.61 (t, *J* = 6.2 Hz, 3H), 3.19 (d, *J* = 6.1 Hz, 2H), 3.16 – 2.98 (m, 2H), 2.46 (d, *J* = 13.9 Hz, 1H), 2.24 – 2.09 (m, 1H), 1.42 (s, 11H). ^{13}C NMR (125 MHz, $CDCl_3$) δ 173.1, 156.3, 156.0, 143.9, 141.7, 127.97, 127.31, 125.3, 120.4, 79.9, 67.8, 56.9, 53.3, 52.2, 51.3, 47.9, 38.6, 28.8, 18.6. **HRMS**: (ESI) calcd for $C_{27}H_{34}N_2O_8S$ $[M + H]^+$ 547.2114; found 547.2118.

(*S*)-2-Amino-4-bromobutanoic acid HBr (41)—L-Homoserine was added to solution of 30% HBr/AcOH in a tube and the tube was sealed tightly and then stirred for 12 h at 50 °C in a heated oil bath. The tube was removed from the oil bath and allowed to warm to room temperature. After careful removal of the seal, the crude product was filtered, washed with EtOAc, and dried under vacuum. The product was obtained as a white powder (78% yield): m.p. of 173–181°C. ^{1}H NMR (500 MHz, CD_3OD) δ 4.01 (t, *J* = 6.7 Hz, 1H), 3.50–3.47 (m 2H), 2.36 (m, 1H), 2.21 (m, 1H); ^{13}C NMR (125 MHz, CD_3OD) δ 171.0, 52.5, 34.7, 28.3.

Methyl *N*-(((9H-fluoren-9-yl)methoxy)carbonyl)-*S*-(4-((tertbutoxycarbonyl)amino)phenyl)homocysteinate (45)—To a solution of **41** (1.04 g, 4.0 mmol) in methanol (95 mL) was carefully added thionyl chloride (0.59 mL, 16.0 mmol, 4 equiv.) drop wise over 30 min. The reaction was stirred under nitrogen overnight, and then it was concentrated under reduced pressure to yield a yellow solid (1.1 g, quantitative yield). It was used in the next step without further purification.

The above ester product was placed in a round bottom flask and an ice-chilled 2:1 mixture of H_2O:DCM containing $NaHCO_3$ (808 mg, 9.6 mmol, 2.4 equiv) was added. Fmoc-Cl (1.2 g, 4.67 mmol, 1.17 equiv.) was added to the reaction mixture portion wise and the reaction was stirred overnight at room temperature. The mixture was separated; the organic layer was collected and the aqueous layer was acidified (pH 1–2) and then extracted with dichloromethane (2×). The organic layers were combined, dried using anhydrous sodium sulfate and evaporated. The product **42** was used in the next step without further purification (1.57 g, 94% yield).

To a solution of Fmoc-protected compound **42** (35 mg, 0.084 mmol) and *tert*-butyl-*N*-(4sulfanyphenyl)carbamate **44** (23 mg, 0.1 mg, 1.2 eq.) in DMF at 0 ^oC was added Cs_2CO_3 (33 mg, 0.01 mmol, 1.2 equiv.) and the reaction was stirred for 1 h. The reaction was worked-up by addition of H_2O and extracted with ethyl acetate (3×). The combined organic layer was washed with brine, dried over anhydrous sodium sulfate and evaporated in vacuo. The crude mixture was purified on silica gel column chromatography (0–20% ethyl acetate/DCM) to produce pure sulfide **45** as a colorless oil (41 mg, yield 87%). $[\alpha]_D^{22}$ + 65.8 (*c* 1.2, $CHCl_3$). ^1H NMR (500 MHz, $CDCl_3$) δ 7.78 (ddd, *J* = 7.6, 2.2, 1.1 Hz, 2H), 7.63 – 7.58 (m, 2H), 7.42 (tdd, *J* = 7.5, 2.2, 1.2 Hz, 2H), 7.37 – 7.30 (m, 6H), 6.48 (s, 1H), 5.36 (d, *J* = 8.4 Hz, 1H), 4.51 (td, *J* = 8.1, 4.8 Hz, 1H), 4.42 (dt, *J* = 7.2, 3.8 Hz, 2H), 4.23 (t, *J* = 7.0 Hz, 1H), 3.75 (s, 3H), 2.85 (t, *J* = 7.4 Hz, 2H), 2.18 – 2.09 (m, 1H), 1.92 (dd, *J* = 14.3, 7.2 Hz, 1H), 1.52 (s, 9H). ^{13}C NMR (125 MHz, $CDCl_3$) δ 172.6, 156.1, 152.8, 144.0, 143.9, 141.5, 137.8, 132.4, 127.9, 127.3, 125.3, 120.2, 119.3, 81.0, 67.2, 53.2, 52.8, 47.4, 32.5, 31.4, 28.5. **HRMS**: (ESI) calcd for $C_{31}H_{34}N_2O_6S$ $[M + H]^+$ 563.2216; found 563.2219.

General procedure for the synthesis of final product inhibitors—To a solution of dipeptide (96.0 mmol, 1 equiv.) in 1,4-dioxane/H_2O (5 ml, 2:1) was added $LiOH{\cdot}H_2O$ (480 mmol) and the reaction was stirred at room temperature for 1 h. After TLC indicated complete consumption of starting material, the reaction was evaporated and the resulting residue was suspended in H_2O, acidified and extracted with ethyl acetate (3×). The combined organic layer was dried using anhydrous sodium sulfate, filtered and evaporated to obtain the free acid as a white solid. Next, the Boc-protected epoxyketone derivatives (**30a-c**) were dissolved in DCM and TFA and added to the reaction mixture with stirring for 30 min, whereupon it was concentrated under reduced pressure.

The TFA salt of the deprotected epoxyketone (1 equiv.) and the previously prepared free acid (1 equiv) were dissolved in DCM (0.5 M) followed by addition of HBTU (1.1 equiv) and DIPEA (2.5 equiv) at 0 ^oC. The reaction was stirred for 1 h at 0 ^oC and then slowly warmed to room temperature and stirred overnight. The reaction mixture was concentrated under reduced pressure, redissolved in ethyl acetate, washed with 1M HCl, $NaHCO_3$, brine,

dried over anhydrous sodium sulfate and concentrated. The crude product was purified on preparative TLC to yield the final products as colorless oils (yields 65–89%).

As necessary, the previous products were subjected to another round of Boc-deprotection using the same procedure described above and the products were purified on RP-HPLC using a Phenomenex Kinetex C18 column (150 × 3 mm, gradient elution with 20% CH_3CN/H_2O + 0.1% TFA to 80% CH_3CN/H_2O + 0.1% TFA over 30 min, flow 0.6 mL/min) to afford the free amine final product (yields 62–74%)

***tert*-Butyl (2-(((*S*)-3-((*S*)-2-hexanamido-3-methylbutanamido)-4-(((*S*)-4-methyl-1-((*R*)-2methyloxiran-2-yl)-1-oxopentan-2-yl)amino)-4-oxobutyl)sulfonyl)ethyl)carbamate (7-Boc)—**$[\alpha]_D^{22}$ + 29.0 (*c* 0.4, CH_3OH). ^1H NMR (500 MHz, CD_3OD) δ 4.53 (dd, *J* = 7.8, 6.1 Hz, 1H), 4.48 (dd, *J* = 11.0, 2.8 Hz, 1H), 4.08 (d, *J* = 7.7 Hz, 1H), 3.53 (td, *J* = 6.8, 2.0 Hz, 2H), 3.26 (d, *J* = 5.0 Hz, 1H), 3.18 (tdt, *J* = 14.1, 10.9, 7.1 Hz, 2H), 2.93 (d, *J* = 5.1 Hz, 1H), 2.25 (td, *J* = 7.3, 2.8 Hz, 2H), 2.22 – 2.19 (m, 1H), 2.15 – 2.08 (m, 1H), 2.06 – 1.98 (m, 1H), 1.76 – 1.68 (m, 1H), 1.61 (p, *J* = 7.5 Hz, 2H), 1.52 (ddd, *J* = 13.2, 10.1, 2.9 Hz, 1H), 1.47 (s, 2H), 1.39 – 1.27 (m, 4H), 0.96 (d, *J* = 0.9 Hz, 3H), 0.93 (m, 3H), 0.91 (m, 6H). ^{13}C NMR (125 MHz, CD_3OD) δ 208.3, 175.1, 172.4, 171.0, 156.6, 79.2, 59.0, 58.8, 51.8, 51.7, 51.0, 48.9, 38.3, 35.3, 33.8, 31.1, 30.1, 27.3, 25.3, 24.9, 22.3, 22.0, 19.9, 18.3, 17.5, 15.7, 12.9. **HRMS**: (ESI) calcd for $C_{31}H_{56}N_4O_9S$ $[M + H]^+$ 661.3846; found 661.3840.

***N*-((*S*)-1-(((*S*)-4-((2-aminoethyl)sulfonyl)-1-(((*S*)-4-methyl-1-((*R*)-2-methyloxiran-2-yl)-1oxopentan-2-yl)amino)-1-oxobutan-2-yl)amino)-3-methyl-1-oxobutan-2-yl)hexanamide (7)—**$[\alpha]_D^{22}$ + 14.6 (*c* 0.16, CH_3OH). ^1H NMR (500 MHz, CD_3OD) δ 4.55 (dd, *J* = 7.7, 6.1 Hz, 1H), 4.50 (dd, *J* = 11.0, 2.8 Hz, 1H), 4.04 (d, *J* = 7.8 Hz, 1H), 3.49 (td, *J* = 3.5, 1.2 Hz, 2H), 3.29 – 3.25 (m, 2H), 3.25 (d, *J* = 2.9 Hz, 1H), 2.94 (d, *J* = 2.5 Hz, 1H), 2.32 – 2.21 (m, 2H), 2.19 – 2.11 (m, 1H), 2.06 – 1.96 (m, 1H), 1.73 (dtd, *J* = 10.8, 6.9, 4.1 Hz, 1H), 1.62 (q, *J* = 7.3 Hz, 2H), 1.58 – 1.51 (m, 1H), 1.48 (s, 3H), 1.42 – 1.26 (m, 7H), 1.01 – 0.88 (m, 15H). ^{13}C NMR (125 MHz, CD_3OD) δ 208.5, 175.2, 172.5, 170.8, 59.3, 58.8, 51.8, 51.3, 50.8, 48.9, 48.9, 38.3, 35.3, 32.9, 31.1, 30.0, 25.3, 24.9, 24.4, 22.2, 22.0, 19.8, 18.2, 17.6, 15.6, 12.8. **HRMS**: (ESI) calcd for $C_{26}H_{48}N_4O_7S$ $[M + H]^+$ 561.3322; found 561.3339.

***tert*-Butyl (2-(((*S*)-4-(((*S*)-4-methyl-1-((*R*)-2-methyloxiran-2-yl)-1-oxopentan-2-yl)amino)-4oxo-3-((*S*)-3-phenyl-2-(2-phenylacetamido)propanamido)butyl)sulfonyl)ethyl)carbamate (8-Boc)—**+ 16.5 (*c* 0.6, $CHCl_3$). ^1H NMR (500 MHz, $CDCl_3$) δ 7.30 (d, *J* = 6.9 Hz, 2H), 7.20 (t, *J* = 3.1 Hz, 2H), 7.14 – 7.11 (m, 2H), 7.05 (d, *J* = 7.1 Hz, 2H), 6.98 – 6.90 (m, 2H), 6.14 (d, *J* = 7.2 Hz, 1H), 5.60 (s, 1H), 4.64 (q, *J* = 7.1 Hz, 1H), 4.61 – 4.54 (m, 3H), 4.48 (ddd, *J* = 10.5, 7.2, 2.9 Hz, 1H), 3.62 (p, *J* = 8.2, 7.1 Hz, 3H), 3.52 (d, *J* = 6.1 Hz, 2H), 3.30 (d, *J* = 5.1 Hz, 1H), 3.24 (q, *J* = 7.4, 6.8 Hz, 3H), 3.02 – 2.91 (m, 2H), 2.89 (d, *J* = 5.0 Hz, 1H), 2.01 (s, 3H), 1.67 (s, 2H), 1.51 (s, 4H), 1.44 (s, 9H), 1.30 (ddd, *J* = 14.2, 10.6, 4.2 Hz, 1H), 0.95 (d, *J* = 6.6 Hz, 8H). ^{13}C NMR (125 MHz, $CDCl_3$) δ 208.9, 171.8, 171.0, 170.1, 156.0, 136.0, 134.4, 129.6, 129.2, 129.2, 128.9, 127.6, 127.2, 80.3, 59.5, 54.7, 53.0, 52.7, 51.4, 51.0, 49.3,

43.5, 39.3, 37.5, 34.6, 28.5, 25.5, 23.5, 21.3, 17.0. **HRMS**: (ESI) calcd for $C_{37}H_{52}N_4O_9S$ $[M + Na]^+$ 751.3353; found 751.3358.

(*S*)-4-((2-Aminoethyl)sulfonyl)-*N*-((S)-4-methyl-1-((*R*)-2-methyloxiran-2-yl)-1-oxopentan-2yl)-2-((*S*)-3-phenyl-2-(2-phenylacetamido)propanamido)butanamide (8)—$[\alpha]_D^{22}$ + 2.5 (*c* 0.5, CH_3OH). ^1H NMR (500 MHz, CD_3OD) δ 7.29 – 7.17 (m, 8H), 7.17 – 7.13 (m, 2H), 4.54–4.49 (m, 2H), 4.46 (dd, *J* = 10.9, 2.8 Hz, 1H), 3.77–369 (m, 4H), 3.51 (d, *J* = 3.4 Hz, 2H), 3.28 – 3.21 (m, 4H), 3.10 (dd, *J* = 13.9, 5.7 Hz, 1H), 2.95 (d, *J* = 5.2 Hz, 1H), 2.93 (s, 1H), 2.23 (ddt, *J* = 14.0, 7.0, 4.3 Hz, 1H), 2.16 – 2.07 (m, 1H), 1.75 (ddt, *J* = 13.7, 6.9, 3.9 Hz, 1H), 1.54 (ddd, *J* = 13.1, 10.0, 2.7 Hz, 1H), 1.48 (s, 3H), 0.97 (dd, *J* = 11.2, 6.6 Hz, 6H. ^{13}C NMR (125 MHz, CD_3OD) δ 208.59, 172.89, 172.29, 170.78, 136.77, 135.29, 128.85, 128.82, 128.27, 128.18, 126.55, 126.49, 58.96, 55.18, 51.88, 51.35, 50.89, 48.88, 48.76, 41.94, 38.20, 36.92, 33.00, 25.07, 24.66, 22.41, 20.02, 15.74. **HRMS**: (ESI) calcd for $C_{37}H_{52}N_4O_9S$ $[M + Na]^+$ 715.3353; found 715.3356. **HRMS**: (ESI) calcd for $C_{32}H_{44}N_4O_7S$ $[M + H]^+$ 629.3009; found 629.3018.

***tert*-Butyl (2-(((*S*)-3-((*S*)-2-hexanamido-3-methylbutanamido)-4-(((*S*)-1-((*R*)-2methyloxiran-2-yl)-1-oxo-3-phenylpropan-2-yl)amino)-4oxobutyl)sulfonyl)ethyl)carbamate (9-Boc)—**+ 6.7 (*c* 0.04, CH_3OH). ^1H NMR (500 MHz, CD_3OD) δ 7.30 – 7.23 (m, 4H), 7.23 – 7.17 (m, 1H), 4.72 (dd, *J* = 9.6, 4.0 Hz, 1H), 4.51 (dd, *J* = 8.0, 5.8 Hz, 1H), 4.02 (d, *J* = 7.7 Hz, 1H), 3.55 – 3.49 (m, 2H), 3.29 (d, *J* = 4.7 Hz, 1H), 3.26 (td, *J* = 6.8, 2.2 Hz, 2H), 3.19 – 3.04 (m, 2H), 2.95 (d, *J* = 5.1 Hz, 1H), 2.70 (dd, *J* = 14.1, 9.6 Hz, 1H), 2.23 (td, *J* = 7.5, 3.0 Hz, 2H), 2.20 – 2.14 (m, 1H), 2.10 – 2.01 (m, 1H), 1.96 (dt, *J* = 13.9, 6.9 Hz, 1H), 1.59 (p, *J* = 7.5 Hz, 2H), 1.48 (dd, *J* = 7.4, 4.0 Hz, 1H), 1.45 (s, 3H), 1.32 (tdd, *J* = 11.7, 9.3, 6.6 Hz, 4H), 0.90 (dt, *J* = 7.2, 3.7 Hz, 6H), 0.83 (d, *J* = 6.8 Hz, 3H). ^{13}C NMR (125 MHz, CD_3OD) δ 207.5, 175.1, 172.3, 170.8, 156.6, 136.6, 128.7, 128.1, 126.5, 79.2, 59.1, 59.0, 53.8, 51.9, 51.7, 50.9, 48.9, 37.4, 35.6, 35.2, 31.1, 30.0, 27.3, 25.2, 22.0, 18.3, 17.6, 15.4, 12.9. **HRMS**: (ESI) calcd for $C_{34}H_{54}N_4O_9S$ $[M + H]^+$ 695.3690; found 695.3693.

***N*-((*S*)-1-(((*S*)-4-((2-Aminoethyl)sulfonyl)-1-(((*S*)-1-((*R*)-2-methyloxiran-2-yl)-1-oxo-3phenylpropan-2-yl)amino)-1-oxobutan-2-yl)amino)-3-methyl-1-oxobutan-2-yl)hexanamide (9)—**$[\alpha]_D^{22}$ + 12.3 (*c* 0.8, CH_3OH). ^1H NMR (500 MHz, CD_3OD) δ 7.29 – 7.23 (m, 4H), 7.22 – 7.18 (m, 1H), 4.73 (dd, *J* = 9.5, 3.9 Hz, 1H), 4.53 (dd, *J* = 7.9, 5.7 Hz, 1H), 3.97 (d, *J* = 7.8 Hz, 1H), 3.48 – 3.46 (m, 4H), 3.28 (d, *J* = 5.1 Hz, 1H), 3.23 (ddd, *J* = 10.3, 8.5, 5.6 Hz, 2H), 3.14 (dd, *J* = 14.1, 4.0 Hz, 1H), 2.96 (d, *J* = 5.1 Hz, 1H), 2.70 (dd, *J* = 14.1, 9.5 Hz, 1H), 2.28 – 2.20 (m, 3H), 2.16 – 2.07 (m, 1H), 1.99 – 1.92 (m, 1H), 1.60 (q, *J* = 7.3 Hz, 3H), 1.46 (s, 3H), 1.37 – 1.30 (m, 4H), 1.01 – 0.99 (m, 1H), 0.91 (dd, *J* = 6.8, 1.8 Hz, 6H), 0.83 (d, *J* = 6.8 Hz, 3H). ^{13}C NMR (125 MHz, CD_3OD) δ 207.7, 175.3, 172.5, 170.7, 136.5, 128.7, 128.1, 126.5, 59.4, 59.0, 54.0, 51.9, 50.8, 49.0, 48.9, 35.6, 35.2, 32.9, 31.1, 29.8, 25.3, 24.5, 21.9, 18.3, 17.6, 15.4, 12.8. **HRMS**: (ESI) calcd for $C_{29}H_{46}N_4O_7S$ $[M + H]^+$ 595.3165; found 595.3149.

***tert*-Butyl (2-(((*S*)-4-(((*S*)-1-((*R*)-2-methyloxiran-2-yl)-1-oxo-3-phenylpropan-2-yl)amino)-4oxo-3-((*S*)-3-phenyl-2-(2-phenylacetamido)propanamido)butyl)sulfonyl)ethyl)carbamate (10-Boc)—** + 36.2 (*c* 0.34, $CHCl_3$). ^{1}H NMR (500 MHz, CD_3CN) δ 7.34 (s, 1H), 7.34 – 7.29 (m, 2H), 7.29 – 7.25 (m, 5H), 7.23 (dd, *J* = 5.0, 1.9 Hz, 4H), 7.14 (m, 4H), 6.80 (d, *J* = 7.3 Hz, 1H), 7.01 (d, *J* = 7.5 Hz, 1H), 5.72 (s, 1H), 4.67 (ddd, *J* = 9.1, 7.1, 4.1 Hz, 1H), 4.47 (d, *J* = 6.8 Hz, 1H), 4.41 (dt, *J* = 8.2, 4.1 Hz, 1H), 3.56 – 3.38 (m, 4H), 3.28 (d, *J* = 5.0 Hz, 1H), 3.15 (dd, *J* = 12.1, 5.7 Hz, 2H), 3.11 – 3.06 (m, 1H), 3.03 – 2.98 (m, 1H), 2.97 (d, *J* = 5.0 Hz, 1H), 2.87 (dd, *J* = 14.0, 8.9 Hz, 1H), 2.76 – 2.67 (m, 1H), 2.23 (m, 1H), 2.16 (ddt, *J* = 15.3, 10.9, 6.3 Hz, 1H), 1.97 (p, *J* = 2.5 Hz, 2H), 1.47 (s, 3H), 1.44 (s, 9H). ^{13}C NMR (125 MHz, CD_3CN) δ 207.7, 171.5, 171.2, 170.3, 155.9, 137.3, 137.1, 135.7, 129.5, 129.4, 128.7, 128.7, 128.6, 128.6, 127.1, 127.0, 126.8, 79.2, 59.4, 55.1, 53.9, 52.5, 52.1, 51.2, 49.3, 42.7, 37.0, 36.0, 34.3, 27.8, 24.7, 16.1. **HRMS**: (ESI) calcd for $C_{40}H_{50}N_4O_9S$ $[M + H]^+$ 763.3377; found 763.3378.

(*S*)-4-((2-Aminoethyl)sulfonyl)-*N*-((*S*)-1-((*R*)-2-methyloxiran-2-yl)-1-oxo-3-phenylpropan-2yl)-2-((*S*)-3-phenyl-2-(2-phenylacetamido)propanamido)butanamide (10)—$[\alpha]_D^{22}$ + 96.5 (*c* 0.36, CH_3OH). ^{1}H NMR (500 MHz, CD_3OD) δ 8.30 (d, *J* = 6.8 Hz, 1H), 8.08 (d, *J* = 8.0 Hz, 1H), 7.34 – 7.18 (m, 10H), 7.12 (td, *J* = 10.3, 9.2, 6.0 Hz, 6H), 4.66 (dd, *J* = 9.8, 3.7 Hz, 1H), 4.50 – 4.38 (m, 2H), 3.53 – 3.44 (m, 2H), 3.27–3.37 (m, 4H), 3.17 – 3.10 (m, 4H), 2.97 (dd, *J* = 7.8, 5.8 Hz, 2H), 2.86 (dd, *J* = 13.8, 9.2 Hz, 1H), 2.66 (dd, *J* = 14.0, 9.9 Hz, 1H), 2.20 (dq, *J* = 14.0, 7.2 Hz, 1H), 2.05 (dt, *J* = 14.5, 7.8 Hz, 1H), 1.47 (s, 3H). ^{13}C NMR (125 MHz, $CDCl_3$) δ 211.52, 176.67, 176.09, 174.36, 140.69, 140.40, 139.08, 132.64, 132.59, 132.52, 132.04, 132.03, 131.93, 130.44, 130.31, 130.23, 62.90, 59.12, 58.13, 55.78, 54.52, 52.63, 52.52, 45.64, 40.68, 39.17, 36.74, 28.37, 19.31. **HRMS**: (ESI) calcd for $C_{35}H_{42}N_4O_7S$ $[M + H]^+$ 663.2852; found 663.2868.

***tert*-Butyl (4-(((*S*)-3-((*S*)-2-hexanamido-3-methylbutanamido)-4-(((*S*)-4-methyl-1-((*R*)-2methyloxiran-2-yl)-1-oxopentan-2-yl)amino)-4-oxobutyl)sulfonyl)phenyl)carbamate (13Boc)—**$[\alpha]_D^{22}$ + 31.6 (*c* 0.23, $CHCl_3$). ^{1}H NMR (500 MHz, $CDCl_3$) δ 7.81 (dd, *J* = 8.9, 2.1 Hz, 2H), 7.58 (dd, *J* = 8.8, 2.2 Hz, 2H), 7.25 (d, *J* = 7.9 Hz, 1H), 7.17 (d, *J* = 7.4 Hz, 2H), 6.43 (dd, *J* = 8.3, 2.1 Hz, 1H), 4.74 (qd, *J* = 7.1, 2.1 Hz, 1H), 4.49 (ddd, *J* = 10.3, 7.6, 3.0 Hz, 1H), 4.30 (ddd, *J* = 8.5, 6.6, 2.0 Hz, 1H), 3.42 – 3.31 (m, 1H), 3.28 (dd, *J* = 5.1, 2.0 Hz, 1H), 3.16 (dt, *J* = 14.3, 7.0 Hz, 1H), 2.89 (dd, *J* = 5.0, 2.1 Hz, 1H), 2.22 (t, *J* = 8.0 Hz, 2H), 2.16 – 2.00 (m, 5H), 1.63 (m, 3H), 1.53 (d, *J* = 2.1 Hz, 9H), 1.51 (d, *J* = 2.1 Hz, 3H), 1.37 – 1.21 (m, 4H), 0.90 (ddt, *J* = 13.3, 8.0, 3.4 Hz, 15H). ^{13}C NMR (125 MHz, $CDCl_3$) δ 208.5, 174.0, 171.7, 170.4, 152.3, 144.1, 131.8, 129.7, 118.3, 81.8, 59.5, 58.5, 52.7, 52.5, 51.3, 51.1, 39.4, 38.8, 36.7, 31.6, 31.2, 28.4, 25.6, 25.4, 23.5, 22.5, 21.3, 19.4, 18.3, 17.0, 14.1. **HRMS**: (ESI) calcd for $C_{35}H_{56}N_4O_9S$ $[M + H]^+$ 709.3846; found 709.3856.

***N*-((*S*)-1-(((*S*)-4-((4-Aminophenyl)sulfonyl)-1-(((*S*)-4-methyl-1-((*R*)-2-methyloxiran-2-yl)-1oxopentan-2-yl)amino)-1-oxobutan-2-yl)amino)-3-methyl-1-oxobutan-2-yl)hexanamide (13)—**$[\alpha]_D^{22}$ + 16.3 (*c* 0.09, $CHCl_3$). ^{1}H NMR (500 MHz,

$CDCl_3$) δ 7.73 – 7.64 (m, 1H), 7.11 (d, *J* = 7.4 Hz, 1H), 7.01 (d, *J* = 7.7 Hz, 1H), 6.79 – 6.67 (m, 2H), 6.10 (d, *J* = 8.3 Hz, 1H), 4.74 (q, *J* = 7.1 Hz, 1H), 4.52 (ddd, *J* = 10.5, 7.4, 3.1 Hz, 1H), 4.32 – 4.22 (m, 3H), 3.41 (ddd, *J* = 14.5, 8.4, 6.2 Hz, 1H), 3.31 (d, *J* = 5.1 Hz, 1H), 3.12 (dt, *J* = 14.5, 6.2 Hz, 1H), 2.90 (d, *J* = 5.0 Hz, 1H), 2.29 – 2.21 (m, 2H), 2.15 (dq, *J* = 22.6, 7.1, 6.6 Hz, 1H), 2.06 (dt, *J* = 14.6, 7.1 Hz, 1H), 1.81 – 1.56 (m, 4H), 1.52 (s, 3H), 1.43 – 1.24 (m, 4H), 1.02 – 0.85 (m, 15H). ^{13}C NMR (125 MHz, $CDCl_3$) δ 208.3, 173.8, 171.4, 170.4, 151.8, 130.5, 126.4, 114.4, 59.5, 58.6, 52.7, 51.3, 51.1, 39.5, 36.8, 31.6, 31.0, 26.0, 25.5, 25.4, 23.5, 22.6, 21.3, 19.4, 18.2, 17.0, 14.2. **HRMS**: (ESI) calcd for $C_{30}H_{48}N_4O_7S$ $[M + H]^+$ 609.3322; found 609.3320.

(*S*)-2-((*S*)-2-Hexanamido-3-methylbutanamido)-*N*1,*N*5-bis((*S*)-4-methyl-1-((*R*)-2methyloxiran-2-yl)-1-oxopentan-2-yl)pentanediamide (14)—$[\alpha]_D^{22}$ + 8.5 (*c* 0.12, $CHCl_3$). ^{1}H NMR (500 MHz, $CDCl_3$) δ 8.17 (d, *J* = 7.1 Hz, 1H), 7.81 (d, *J* = 7.3 Hz, 1H), 6.19 (d, *J* = 7.7 Hz, 1H), 6.04 (d, *J* = 8.7 Hz, 1H), 4.58 (ddt, *J* = 11.5, 7.2, 2.2 Hz, 1H), 4.52 (ddt, *J* = 11.3, 7.1, 2.2 Hz, 1H), 4.21 (ddd, *J* = 8.6, 6.7, 1.6 Hz, 1H), 4.19 – 4.11 (m, 0H), 3.50 (d, *J* = 5.1 Hz, 1H), 3.47 (d, *J* = 5.2 Hz, 1H), 2.99 – 2.90 (m, 2H), 2.30 (dt, *J* = 14.3, 4.4 Hz, 1H), 2.24 – 2.16 (m, 2H), 2.11 (dq, *J* = 8.7, 6.1, 4.3 Hz, 1H), 2.01 (ddd, *J* = 12.9, 6.1, 3.5 Hz, 1H), 1.98 – 1.85 (m, 1H), 1.77 (td, *J* = 12.2, 6.2 Hz, 1H), 1.71 – 1.56 (m, 6H), 1.53 (dd, *J* = 3.5, 1.6 Hz, 6H), 1.36 – 1.22 (m, 4H), 1.20 – 1.10 (m, 1H), 1.02 – 0.92 (m, 12H), 0.90 (d, *J* = 6.6 Hz, 9H). ^{13}C NMR (125 MHz, $CDCl_3$) δ 212.8, 212.6, 173.2, 172.7, 171.5, 170.6, 59.8, 59.6, 58.1, 53.3, 53.1, 52.1, 51.8, 51.5, 38.8, 38.7, 36.9, 31.8, 31.7, 31.6, 28.5, 25.6, 25.4, 23.6, 23.5, 22.6, 21.1, 20.8, 19.1, 18.4, 17.0, 16.9, 14.1. **HRMS**: (ESI) calcd for $C_{34}H_{58}N_4O_8$ $[M + H]^+$ 651.4333; found 651.4338.

(*S*)-2-((*S*)-3-(4-Aminophenyl)-2-hexanamidopropanamido)-*N*1,*N*5-bis((*S*)-4-methyl-1-((*R*)2-methyloxiran-2-yl)-1-oxopentan-2-yl)pentanediamide (15)—$[\alpha]_D^{22}$ + 18.9 (*c* 0.42, $CHCl_3$). ^{1}H NMR (500 MHz, $CDCl_3$) δ 8.11 (d, *J* = 6.7 Hz, 1H), 7.72 (d, *J* = 7.0 Hz, 1H), 7.04 – 6.85 (m, 2H), 6.65 – 6.54 (m, 2H), 6.25 (d, *J* = 7.4 Hz, 1H), 5.97 (d, *J* = 7.5 Hz, 1H), 4.60 – 4.44 (m, 3H), 4.09 (ddd, *J* = 12.0, 7.4, 4.9 Hz, 1H), 3.69 – 3.58 (m, 2H), 3.52 (d, *J* = 5.2 Hz, 1H), 3.49 (d, *J* = 5.1 Hz, 1H), 2.95 (t, *J* = 5.4 Hz, 2H), 2.91 (t, *J* = 6.8 Hz, 2H), 2.25 (dt, *J* = 14.0, 3.7 Hz, 1H), 2.12 (td, *J* = 7.4, 3.3 Hz, 2H), 2.07 – 1.94 (m, 2H), 1.87 (ddp, *J* = 9.6, 6.5, 3.3, 2.9 Hz, 2H), 1.60 – 1.52 (m, 6H), 1.53 (s, 3H), 1.52 (s, 3H), 1.33 – 1.20 (m, 4H), 1.19 – 1.10 (m, 1H), 1.02 – 0.94 (m, 12H), 0.87 (t, *J* = 7.2 Hz, 3H). ^{13}C NMR (125 MHz, $CDCl_3$) δ 215.3, 212.5, 173.0, 172.5, 171.1, 170.2, 145.2, 130.1, 126.1, 115.3, 59.5, 59.4, 54.0, 53.1, 52.9, 51.8, 51.5, 51.5, 38.7, 38.6, 37.2, 36.5, 31.5, 31.3, 28.4, 25.3, 25.2, 25.1, 23.4, 23.3, 22.3, 21.0, 20.9, 16.8, 16.6, 13.8. **HRMS**: (ESI) calcd for $C_{38}H_{59}N_5O_8$ $[M + H]^+$ 714.4442; found 714.4470.

(*S*)-2-((*S*)-2-(2-(4-Aminophenyl)acetamido)-3-methylbutanamido)-*N*1,*N*5-bis((*S*)-4-methyl1-((*R*)-2-methyloxiran-2-yl)-1-oxopentan-2-yl)pentanediamide (16)—$[\alpha]_D^{22}$ + 62.5 (*c* 0.52, $CHCl_3$). ^{1}H NMR (500 MHz, $CDCl_3$) δ 8.10 (d, *J* = 7.0 Hz, 1H), 7.78 (d, *J* = 7.2 Hz, 1H), 7.04 (dd, *J* = 8.7, 2.5 Hz, 2H), 6.67 (dd, *J* = 8.6, 2.4 Hz, 2H), 6.30 (d, *J* = 7.7 Hz, 1H), 5.91 (d, *J* = 8.7 Hz, 1H), 4.55 (dddt, *J* = 21.1, 10.1, 7.0, 2.8 Hz, 2H), 4.21 – 4.07 (m, 2H), 3.67 (bs, 2H), 3.54 – 3.41 (m, 4H), 2.95 (dd, *J* = 5.1, 2.1 Hz, 2H), 2.29 (dt, *J* = 14.3, 4.2 Hz, 1H), 2.10 (ddt, *J* = 12.7, 9.1, 4.3 Hz, 1H), 2.05 – 1.85 (m, 2H),

1.79 – 1.71 (m, 1H), 1.60 – 1.54 (m, 4H), 1.53 (s, 3H), 1.52 (s, 3H), 1.29 – 1.21 (m, 1H), 1.16 (ddd, *J* = 14.3, 11.1, 3.8 Hz, 1H), 0.96 (m, 12H), 0.83 (d, *J* = 6.6 Hz, 3H), 0.76 (d, *J* = 6.6 Hz, 3H). ^{13}C NMR (125 MHz, $CDCl_3$) δ 212.5, 212.3, 172.5, 171.8, 171.3, 170.0, 145.6, 130.3, 124.1, 115.6, 59.5, 59.4, 58.2, 53.1, 52.9, 51.8, 51.5, 51.2, 42.8, 38.6, 38.5, 31.6, 30.8, 28.3, 25.3, 25.1, 23.4, 23.2, 20.9, 20.6, 19.0, 17.9, 16.8, 16.6. **HRMS**: (ESI) calcd for $C_{36}H_{56}N_5O_8$ $[M + H]^+$ 686.4129; found 686.4119.

Methyl 4-((4-aminophenyl)sulfonyl)-2-((*S*)-2-((*S*)-2-hexanamido-3-methylbutanamido)-5(((*S*)-4-methyl-1-((*R*)-2-methyloxiran-2-yl)-1-oxopentan-2-yl)amino)-5oxopentanamido)butanoate (17)—$[\alpha]_D^{22}$ + 6.5 (*c* 0.14, $CHCl_3$). ^{1}H NMR (500 MHz, CD_3OD) δ 7.57 (dd, *J* = 9.0, 2.2 Hz, 2H), 6.76 (d, *J* = 8.8 Hz, 2H), 4.54 (ddd, *J* = 17.2, 10.2, 3.9 Hz, 2H), 4.19 (t, *J* = 7.3 Hz, 1H), 4.10 (dd, *J* = 7.5, 2.5 Hz, 1H), 3.72 (s, 3H), 3.29 (d, *J* = 5.4 Hz, 1H), 3.25 – 3.13 (d, *J* = 5.1 Hz, 2H), 2.94 (d, *J* = 5.1 Hz, 1H), 2.34 – 2.21 (m, 5H), 2.04 – 1.95 (m, 3H), 1.94 – 1.86 (m, 1H), 1.71 (m, 1H), 1.65 – 1.58 (m, 3H), 1.51 – 1.45 (m, 1H), 1.47 (s, 3H), 1.38 – 1.27 (m, 4H), 0.92 (m, 15H). ^{13}C NMR (125 MHz, CD_3OD) δ 209.3, 175.0, 173.5, 172.4, 172.2, 171.7, 129.7, 129.0, 124.3, 113.5, 58.8, 52.6, 52.4, 51.8, 51.8, 50.8, 50.8, 50.7, 38.4, 35.4, 31.1, 30.9, 30.3, 27.2, 27.1, 25.2, 24.9, 24.9, 19.9, 18.3, 17.5, 15.6, 15.6, 12.9. **HRMS**: (ESI) calcd for $C_{36}H_{57}N_5O_{10}S$ $[M + H]^+$ 752.3904; found 752.3910.

Analytical data for analogue 22—$[\alpha]_D^{22}$ + 28.7 (*c* 0.04, $CHCl_3$). ^{1}H NMR (500 MHz, CD_3OD) δ 7.67 (d, *J* = 7.4 Hz, 1H), 7.49 (dd, *J* = 6.2, 3.6 Hz, 1H), 7.46 (m, 3H), 7.40 – 7.31 (m, 2H), 7.27 (dd, *J* = 7.3, 1.6 Hz, 1H), 5.15 (dd, *J* = 14.0, 2.3 Hz, 1H), 4.57 – 4.43 (m, 2H), 4.10 (dd, *J* = 7.6, 3.7 Hz, 1H), 3.71 (d, *J* = 14.0 Hz, 1H), 3.57 (q, *J* = 6.4 Hz, 2H), 3.25 (m, 3H), 3.19 – 3.11 (m, 2H), 2.92 (d, *J* = 5.1 Hz, 1H), 2.29 – 2.18 (m, 4H), 2.16 – 2.09 (m, 1H), 1.98 (d, *J* = 6.6 Hz, 2H), 1.60 (p, *J* = 7.6 Hz, 2H), 1.56 – 1.48 (m, 1H), 1.46 (s, 3H), 1.41 – 1.23 (m, 12H), 0.99 – 0.85 (m, 15H). **HRMS**: (ESI) calcd for $C_{47}H_{65}N_5O_9S$ $[M + H]^+$ 875.4503; found 875.4511.

Analytical data for analogue 23—$[\alpha]_D^{22}$ + 2.5 (*c* 0.001, MeOH). ^{1}H NMR (500 MHz, CD_3OD) δ 7.85 – 7.79 (d, *J* = 7.8 Hz, 2H), 7.74 – 7.69 (d, *J* = 8.7 Hz, 2H), 7.64 (d, *J* = 7.5 Hz, 1H), 7.61 – 7.57 (d, *J* = 8.7 Hz, 2H), 7.487.42 (m, 3H), 7.38 (d, *J* = 7.8 Hz, 2H), 7.35 – 7.30 (m, 3H), 7.24 (t, *J* = 6.2 Hz, 1H), 5.17 (s, 2H), 5.12 (dd, *J* = 14.0, 3.0 Hz, 1H), 4.49 – 4.40 (m, 3H), 4.07 (dd, *J* = 11.8, 7.5 Hz, 2H), 3.69 (d, *J* = 14.0 Hz, 1H), 3.45 (p, *J* = 1.5 Hz, 1H), 3.28 – 3.22 (m, 4H), 3.21 (d, *J* = 5.3 Hz, 1H), 3.17 (p, *J* = 1.6 Hz, 1H), 3.07 (dd, *J* = 13.4, 6.7 Hz, 2H), 2.91 (d, *J* = 5.1 Hz, 1H), 2.22 (td, *J* = 7.4, 2.2 Hz, 4H), 2.13–2.10 (m, 1H), 2.06 (m, 4H), 2.00 (tt, *J* = 13.3, 6.8 Hz, 2H), 1.58 (p, *J* = 7.6 Hz, 2H), 1.47 (s, 3H), 1.40 – 1.23 (m, 10H), 0.98 – 0.85 (m, 21H). ^{13}C NMR (125 MHz, $CDCl_3$) δ 212.05, 179.02, 178.56, 177.80, 176.47, 176.22, 174.91, 174.77, 164.82, 157.70, 155.46, 148.51, 142.18, 136.04, 135.97, 135.55, 133.04, 132.91, 132.49, 132.44, 132.12, 131.70, 131.40, 130.62, 128.99, 126.83, 126.24, 123.69, 121.73, 111.33, 70.12, 63.14, 62.87, 62.78, 59.14, 57.44, 55.89, 55.70, 55.01, 54.90, 39.25, 38.75, 38.03, 35.06, 34.08, 34.02, 33.29, 32.91, 29.55, 29.22, 28.85, 28.73, 28.68, 26.24, 25.95, 23.83, 22.29, 22.21, 21.40, 19.65, 16.84. **HRMS**: (ESI) calcd for $C_{70}H_{92}N_{10}O_{14}S$ $[M + H]^+$ 1329.6593; found 1329.6611.

4.3. Biological Evaluation

4.3.1. Proteasome Inhibition Assays—Human recombinant 20S proteasome (Enzo Life Sciences; Farmingdale, NY) was assayed using fluorogenic substrates. The chymotrypsin-like, trypsin-like, and caspase-like sites were independently assayed using the selective substrates Suc-LLVY-AMC, Cbz-LLE-AMC, and Cbz-VGR-AMC, respectively (Enzo Life Sciences; Farmingdale, NY). An 11-point, 3-fold serial dilution dose-response assay was performed in triplicate. Inhibitor (10 μL) or vehicle control in 25% DMSO was added to each well of a 96-well plate, followed by 30 μL of assay buffer (100 mM Tris, pH 7.5, EDTA 0.5 mM, SDS 0.03%) containing 3 μg/mL of 20S proteasome. After 30 minutes of incubation at 37°C, 10 μL of 200 μM substrate was added to initiate proteasome reaction, which proceeded for 30 min at 37°C. The resultant dose response concentration range was 1.0 μM to 0.17 nM inhibitor in a 50 μL final reaction volume. The plates were analyzed on a SpecraMax Gemini or SpectraMax M5 microplate reader (PerkinElmer Life Sciences) and the fluorescent signal was measured at the excitation and emission wavelengths of 365 and 450 nm, respectively. Data were scaled to internal controls and a four-parameter logistic model (GraphPad vs. 5.0, Prism) was used to fit the measured data and determine IC_{50} values.

4.3.2. Antibody conjugation reaction of compounds 22 and 23 with trastuzumab.[31]—Compound **22** or **23** were dissolved in DMSO to a concentration of 5 mM. The solution was added to purified trastuzumab that was produced by cell-free synthesis and possessing unique sites for *p*-azidomethylphenylalanine (pAMF) on either HC F404 or LC S7. The antibody was dissolved in PBS buffer to a final compound concentration of 200 μM and a final antibody concentration of 3 mg/mL (20 μM) for a 10:1 molar ratio of compound:antibody. The reaction mixture was incubated at ambient temperature (25 °C) for 16 h and excess compound was removed using Zeba plates (Thermo Scientific) equilibrated in 1× PBS. Drug loading efficiency (i.e. the DAR of the final conjugate) was measured via LC/MS and MALD-TOF spectrometry analysis as described in Currier et al.;[32] drug:antibody ratios (DARs) were 1.22 (HCF404) and 1.71 (LCS7) for the noncleavable **22**-containing ADCs, and 1.94 (HCF404) and 1.79 (LCS7) for the cleavable **23**-containing ADCs.[32] Conjugate purity was determined with an Agilent TapeStation Instrument and concentrations of the final conjugates were determined from their absorption at 280 nm.

4.3.3. Toxicity by CellTiter-Glo® for the ADCs—Cytotoxicity effects of **7-Boc**, **13** and the ADCs were evaluated using a cell proliferation assay. Adherent cancer cell lines SKBR3 (Her2+), MDA-MB-231 (Her2-) and MDA-MB-468 (Her2-) were obtained from ATCC and maintained in high glucose DMEM/F12 (50/50) medium (Cellgro-Mediatech; Manassas, VA) supplemented with 10% heat-inactivated fetal bovine serum (Hyclone; Thermo Scientific; Waltham, MA), 2 mM glutamax (Invitrogen; Carlsbad, CA) and 1× penecillin/streptomycin (Cellgro-Mediatech; Manassas, VA). For adherent cells, a total of 1000 cells in a volume of 40 μl were seeded in a 96-well half area flat bottom white polystyrene plate the day before the assay. Test compounds (**7-Boc**, **13** and the ADCs) were formulated at 2× concentration in culture medium and filtered through MultiScreen HTS 96-Well Filter Plates (Millipore; Billerica, MA). Filter sterilized compounds were serial diluted

in culture medium and 40 μL of the compounds were added into treatment wells. For adherent cells, plates were cultured at 37 °C in a CO_2 incubator for 72 h. For cell viability measurements, 80 μL of Cell Titer-Glo® reagent (Promega Corp.; Madison, WI) was added into each well, and plates processed as per product instructions. Relative luminescence was measured on an ENVISION® plate reader (Perkin-Elmer; Waltham, MA). Relative Luminescent Units (RLU) were converted to percent viability using untreated cells as controls. Data was fitted with non-linear regression analysis, using GraphPad Prism v 5.00. Relative luminescence was measured on an ENVISION® plate reader (Perkin-Elmer; Waltham, MA). Relative luminescence readings were converted to percent viability using untreated cells as controls. Data was fitted with non-linear regression analysis, using GraphPad v 5.00 software (San Diego, CA). Data were expressed as percent relative cell viability vs. dose of compounds in nM. Cell killing IC_{50}'s were calculated by Prism to evaluate the potency of each compound on each cell line. The corresponding heavy- and light-chain ADCs of cleavable ValCitpABmonomethylauristatin were used as a positive control and comparator compound.

4.3.4. Cytotoxicity assay to NCI-H460 human lung carcinoma cells—Human large cell lung carcinoma cells (NCI-H460) were added to 96-well plates at 3.33×10^4 cells/mL in RPMI-1640 media with 10% fetal bovine serum (FBS) and 1% penicillin/streptomycin in a volume of 180 μL per well. The cells were incubated for 24 h (37 ºC, 5% CO_2) to permit recovery before treatment with carmaphycins and their analogs. The pure synthetic compounds and doxorubicin (positive control) were dissolved in DMSO to a stock concentration of 1 mg/mL. Their working solutions were prepared through serial dilutions in RPMI-1640 media without FBS, with 20 μL added to each well to give ten final concentrations in the range between 10 and 0.0003 μg/mL in duplicates. Negative control wells were prepared by adding an equal volume of RPMI 1640 media lacking FBS for each plate; positive control wells were prepared at 1 and 0.1 μg/mL concentrations of doxorubicin. Plates were incubated for 48 h prior to MTT staining. Plates were read with a ThermoElectron Multiskan Ascent plate reader at 570 and 630 nm to define cell viability. Dose-response curves were plotted to determine IC_{50} values using GraphPad Prism 4.

Supplementary Material

Refer to Web version on PubMed Central for supplementary material.

Acknowledgments

We thank J. Hanson, Sutro Bio, for assistance with the design and testing of the ADC and we also thank J. Lee at UCSD for his assistance in cytotoxicity assay of these analogues. We gratefully acknowledge support of this work from NIH CA100851. We thank the CARMABI research station and the country of Curaçao for permission to make the original cyanobacterial collections yielding the carmaphycins. JA thanks the University of Jordan and the Jordanian Scientific Research Support Fund for the scientific research leave support.

References:

[1]. Chudasama V, Maruani A, Caddick S, Recent advances in the construction of antibody–drug conjugates, Nat. Chem (2016). doi:10.1038/nchem.2415.

[2]. Polakis P, Antibody Drug Conjugates for Cancer Therapy, Pharmacol. Rev 68 (2015) 3 LP–19. http://pharmrev.aspetjournals.org/content/68/1/3.abstract.

[3]. Beck A, Goetsch L, Dumontet C, Corvaïa N, Strategies and challenges for the next generation of antibody–drug conjugates, Nat. Rev. Drug Discov 16 (2017) 315–337. doi:10.1038/nrd.2016.268. [PubMed: 28303026]

[4]. Gébleux R, Casi G, Antibody-drug conjugates: Current status and future directions, Pharmacol. Ther (2016). doi:10.1016/j.drudis.2013.11.004.

[5]. Chari RVJ, Miller ML, Widdison WC, Antibody-drug conjugates: An emerging concept in cancer therapy, Angew. Chemie - Int. Ed 53 (2014) 3796–3827. doi:10.1002/anie.201307628.

[6]. Tan L, Filamentous tropical marine cyanobacteria: a rich source of natural products for anticancer drug discovery, J. Appl. Phycol 22 (2010) 659–676. doi:10.1007/s10811-010-9506-x.

[7]. Gerwick WH, Moore BS, Lessons from the past and charting the future of marine natural products drug discovery and chemical biology, Chem. Biol 19 (2012) 85–98. doi:10.1016/j.chembiol.2011.12.014. [PubMed: 22284357]

[8]. Tan LT, Bioactive natural products from marine cyanobacteria for drug discovery, Phytochemistry. 68 (2007) 954–979. doi:10.1016/j.phytochem.2007.01.012. [PubMed: 17336349]

[9]. Nunnery JK, Mevers E, Gerwick WH, Biologically active secondary metabolites from marine cyanobacteria, Curr. Opin. Biotechnol 21 (2010) 787–793. doi:10.1016/j.copbio.2010.09.019. [PubMed: 21030245]

[10]. Pereira AR, Kale AJ, Fenley AT, Byrum T, Debonsi HM, Gilson MK, Valeriote FA, Moore BS, Gerwick WH, The Carmaphycins: New Proteasome Inhibitors Exhibiting an α,β-Epoxyketone Warhead from a Marine Cyanobacterium, ChemBioChem. 13 (2012) 810–817. doi:10.1002/cbic.201200007. [PubMed: 22383253]

[11]. Trivella DBB, Pereira AR, Stein ML, Kasai Y, Byrum T, Valeriote FA, Tantillo DJ, Groll M, Gerwick WH, Moore BS, Enzyme inhibition by hydroamination: Design and mechanism of a hybrid carmaphycin-syringolin enone proteasome inhibitor, Chem. Biol 21 (2014) 782–791. doi:10.1016/j.chembiol.2014.04.010. [PubMed: 24930969]

[12]. Kim KB, Crews CM, From epoxomicin to carfilzomib: chemistry, biology, and medical outcomes, Nat. Prod. Rep 30 (2013) 600. doi:10.1039/c3np20126k. [PubMed: 23575525]

[13]. Kupperman E, Lee EC, Cao Y, Bannerman B, Fitzgerald M, Berger A, Yu J, Yang Y, Hales P, Bruzzese F, Liu J, Blank J, Garcia K, Tsu C, Dick L, Fleming PE, Yu L, Manfredi M, Rolfe M, Bolen J, Evaluation of the proteasome inhibitor MLN9708 in preclinical models of human cancer., Cancer Res. 70 (2010) 1970–1980. doi:10.1158/0008-5472.CAN-09-2766. [PubMed: 20160034]

[14]. Zhou HJ, Aujay MA, Bennett MK, Dajee M, Demo SD, Fang Y, Ho MN, Jiang J, Kirk CJ, Laidig GJ, Lewis ER, Lu Y, Muchamuel T, Parlati F, Ring E, Shenk KD, Shields J, Shwonek PJ, Stanton T, Sun CM, Sylvain C, Woo TM, Yang J, Design and synthesis of an orally bioavailable and selective peptide epoxyketone proteasome inhibitor (PR-047), J. Med. Chem 52 (2009) 3028–3038. doi:10.1021/jm801329v. [PubMed: 19348473]

[15]. Huang X, Dixit VM, Drugging the undruggables: exploring the ubiquitin system for drug development, Cell Res. 26 (2016) 484–498. doi:10.1038/cr.2016.31. [PubMed: 27002218]

[16]. Piva R, Ruggeri B, Williams M, Costa G, Tamagno M, Ferrero D, Giai V, Coscia M, Peola S, Massaia M, Pezzoni G, Allievi C, Pescalli N, Cassin M, Di Giovine S, Nicoli P, De Feudis P, Strepponi I, Roato M, Ferracini R, Bussolati B, Camussi G, Jones-Bolin S, Hunter K, Zhao H, Neri A, Palumbo A, Berkers C, Ovaa H, Bernareggi A, Inghirami G, CEP-18770: A novel, orally active proteasome inhibitor with a tumor-selective pharmacologic profile competitive with bortezomib, Blood. 111 (2008) 2765–2775. doi:10.1182/blood-2007-07100651. [PubMed: 18057228]

[17]. Dou QP, Zonder JA, Overview of proteasome inhibitor-based anti-cancer therapies: perspective on bortezomib and second generation proteasome inhibitors versus future generation inhibitors of ubiquitin-proteasome system., Curr. Cancer Drug Targets 14 (2014) 517–36. doi:10.2174/1568009614666140804154511. [PubMed: 25092212]

[18]. Manasanch EE, Orlowski RZ, Proteasome inhibitors in cancer therapy, Nat Rev Clin Oncol 14 (2017) 417–433. http://dx.doi.org/10.1038/nrclinonc.2016.206. [PubMed: 28117417]

[19]. Mroczkiewicz M, Winkler K, Nowis D, Placha G, Golab J, Ostaszewski R, Studies of the synthesis of all stereoisomers of MG-132 proteasome inhibitors in the tumor targeting approach, J. Med. Chem 53 (2010) 1509–1518. doi:10.1021/jm901619n. [PubMed: 20112914]

[20]. Geurink PP, Van Der Linden WA, Mirabella AC, Gallastegui N, De Bruin G, Blom AEM, Voges MJ, Mock ED, Florea BI, Van Der Marel GA, Driessen C, Van Der Stelt M, Groll M, Overkleeft HS, Kisselev AF, Incorporation of non-natural amino acids improves cell permeability and potency of specific inhibitors of proteasome trypsin-like sites, J. Med. Chem 56 (2013) 1262–1275. doi:10.1021/jm3016987. [PubMed: 23320547]

[21]. Montero A, Beierle JM, Olsen CA, Ghadiri MR, Design, Synthesis, Biological Evaluation, and Structural Characterization of Potent Histone Deacetylase Inhibitors Based on Cyclic alpha/beta-Tetrapeptide Architectures, J. Am. Chem. Soc 131 (2009) 3033–3041. doi:10.1021/Ja809508f. [PubMed: 19239270]

[22]. Yang JY, Sanchez LM, Rath CM, Liu X, Boudreau PD, Bruns N, Glukhov E, Wodtke A, De Felicio R, Fenner A, Wong WR, Linington RG, Zhang L, Debonsi HM, Gerwick WH, Dorrestein PC, Molecular networking as a dereplication strategy, J. Nat. Prod 76 (2013) 1686–1699. doi:10.1021/np400413s. [PubMed: 24025162]

[23]. Adams J, The development of proteasome inhibitors as anticancer drugs, Cancer Cell. 5 (2004) 417–421. doi:10.1016/S1535-6108(04)00120-5. [PubMed: 15144949]

[24]. Mirabella AC, Pletnev AA, Downey SL, Florea BI, Shabaneh TB, Britton M, Verdoes M, Filippov DV, Overkleeft HS, Kisselev AF, Specific cellpermeable inhibitor of proteasome trypsin-like sites selectively sensitizes myeloma cells to bortezomib and carfilzomib, Chem. Biol 18 (2011) 608–618. doi:10.1016/j.chembiol.2011.02.015. [PubMed: 21609842]

[25]. Lu J, Jiang F, Lu A, Zhang G, Linkers having a crucial role in antibody-drug conjugates, Int. J. Mol. Sci 17 (2016). doi:10.3390/ijms17040561.

[26]. Zimmerman ES, Heibeck TH, Gill A, Li X, Murray CJ, Madlansacay MR, Tran C, Uter NT, Yin G, Rivers PJ, Yam AY, Wang WD, Steiner AR, Bajad SU, Penta K, Yang W, Hallam TJ, Thanos CD, Sato AK, Production of site-specific antibody-drug conjugates using optimized non-natural amino acids in a cell-free expression system, Bioconjug. Chem 25 (2014) 351–361. doi:10.1021/bc400490z. [PubMed: 24437342]

[27]. Spangler B, Kline T, Hanson J, Li X, Zhou S, Wells JA, Sato AK, Renslo AR, Toward a Ferrous Iron-Cleavable Linker for Antibody–Drug Conjugates, Mol. Pharm 15 (2018) 2054–2059. doi:10.1021/acs.molpharmaceut.8b00242. [PubMed: 29569925]

[28]. K. Kline T; Yin Q; Bajjuri, Hemiasterlin Derivatives for Conjugation and Therapy. WO 2016/123582 A1, 2016.

[29]. Kelleman A, Mattern RH, Pierschbacher MD, Goodman M, Incorporation of thioether building blocks into an alphavbeta3- specific RGD peptide: synthesis and biological activity, Biopolymers. 71 (2003) 686–695. [PubMed: 14991678]

[30]. Patel SK, Long TE, Preparation of vinylglycines by thermolysis of homocysteine sulfoxides, Tetrahedron Lett. 50 (2009) 5067–5070. doi:10.1016/j.tetlet.2009.06.082.

[31]. Kline T, Yin Q, Bajjuri K, Preparation of hemiasterlin derivatives and their antibody conjugates for use in cancer therapy., 2016.

[32]. Currier NV, Ackerman SE, Kintzing JR, Chen R, Filsinger Interrante M, Steiner A, Sato AK, Cochran JR, Targeted Drug Delivery with an Integrin-Binding Knottin-Fc-MMAF Conjugate Produced by Cell-Free Protein Synthesis, Mol. Cancer Ther 15 (2016) 1291–1300. doi:10.1158/1535-7163.MCT-15-0881. [PubMed: 27197305]

Highlights

- A library of carmaphycin B analogues were synthesized that contain amine handles and thus enabled their attachment to an antibody-linker
- These investigations resulted in identifying the P2 residue in the carmaphycins as the most suitable site for linker attachment point
- The basicity of these incorporated amine handles was shown to strongly impact their cytotoxic properties
- The most potent compound, analogue **13**, showed an IC_{50} of 0.43, 1.8 and 2.6 nM against SKBR3, H460 and HCT116 cells, respectively, and 1.5 nM against the ChT-L site of the proteasome

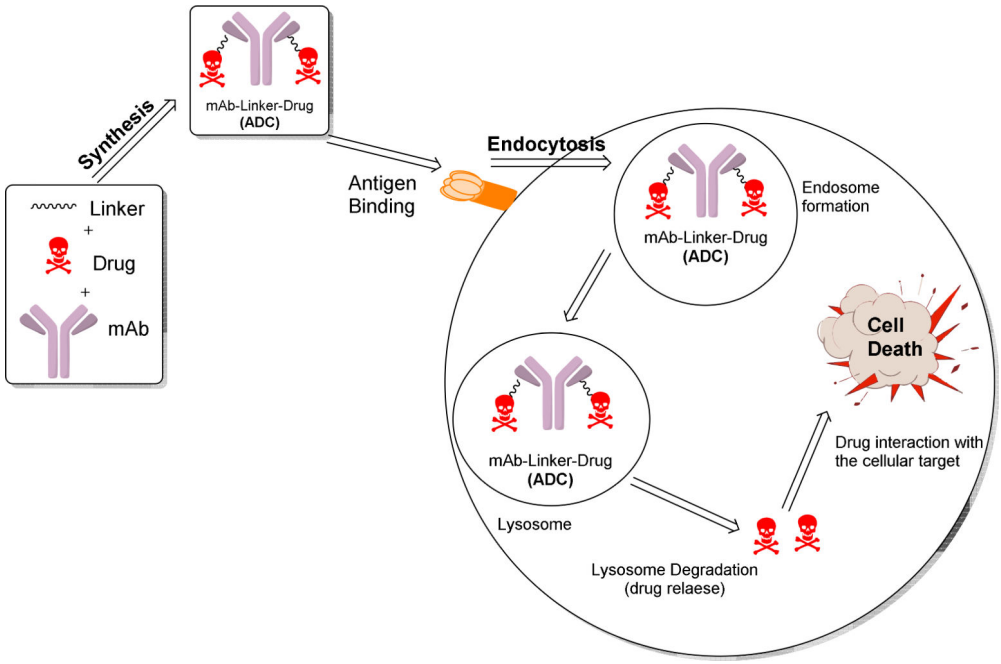

Figure 1.
Overview of the targeted cell killing strategy of ADC based drugs.

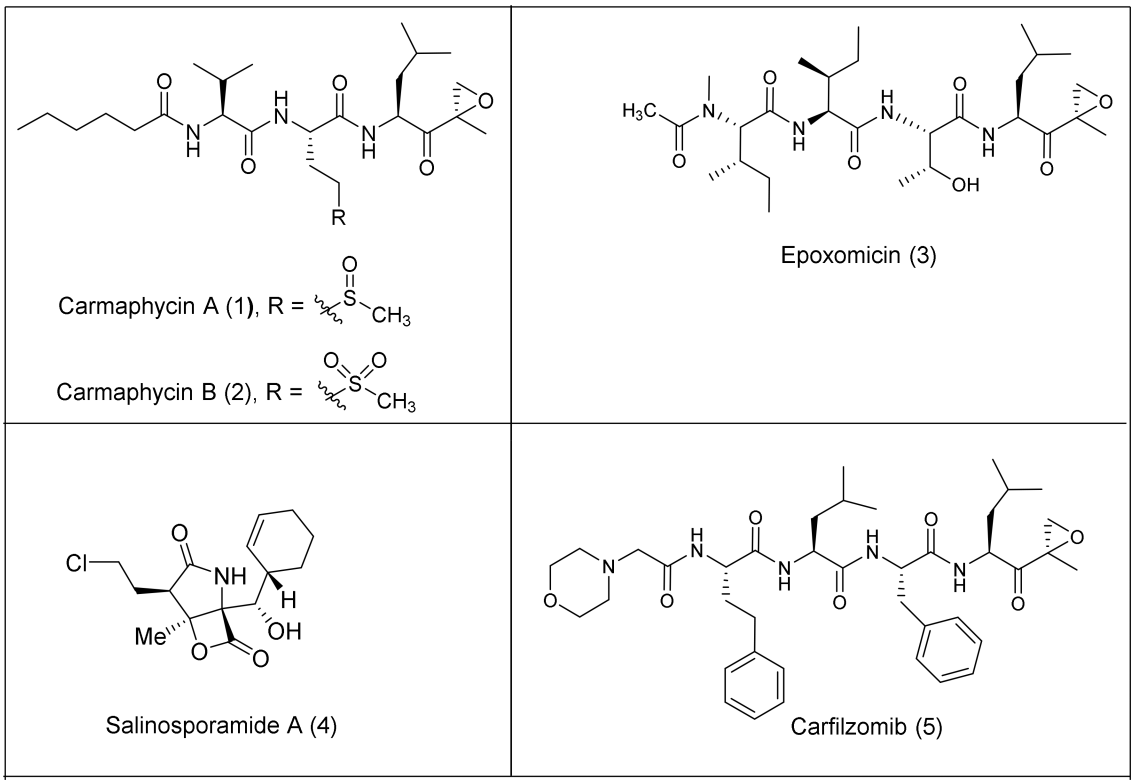

Figure 2.

Structures of carmaphycin A (**1**) and B (**2**), epoxomicin (**3**), salinosporamide A (**4**) and carfilzomib (**5**).

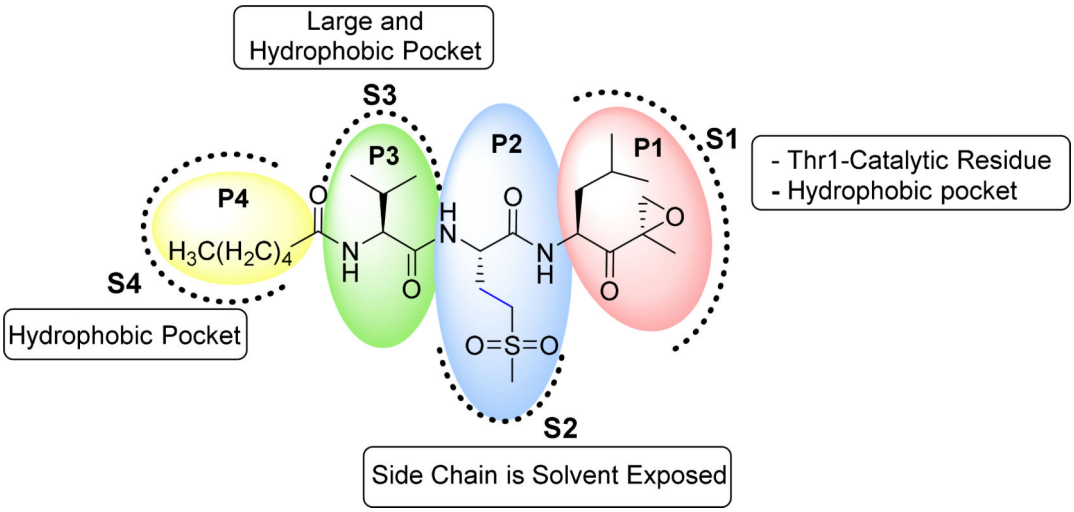

Figure 3.
SAR elements of the carmaphycin B (**2**).

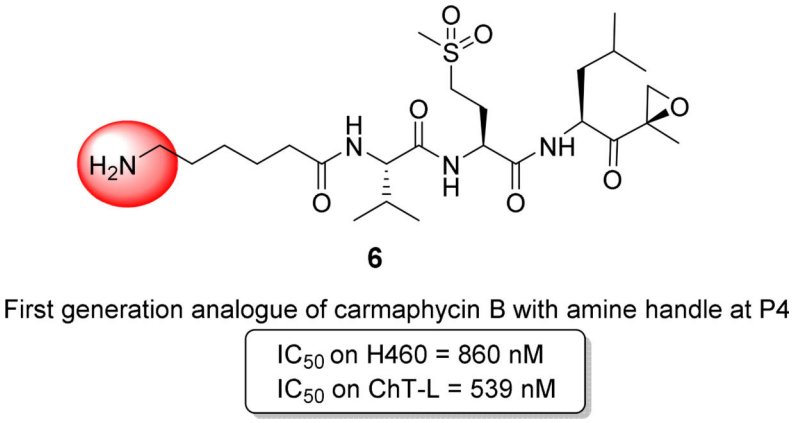

Figure 4.
Structure of first-generation carmaphycin B analogue **6**.

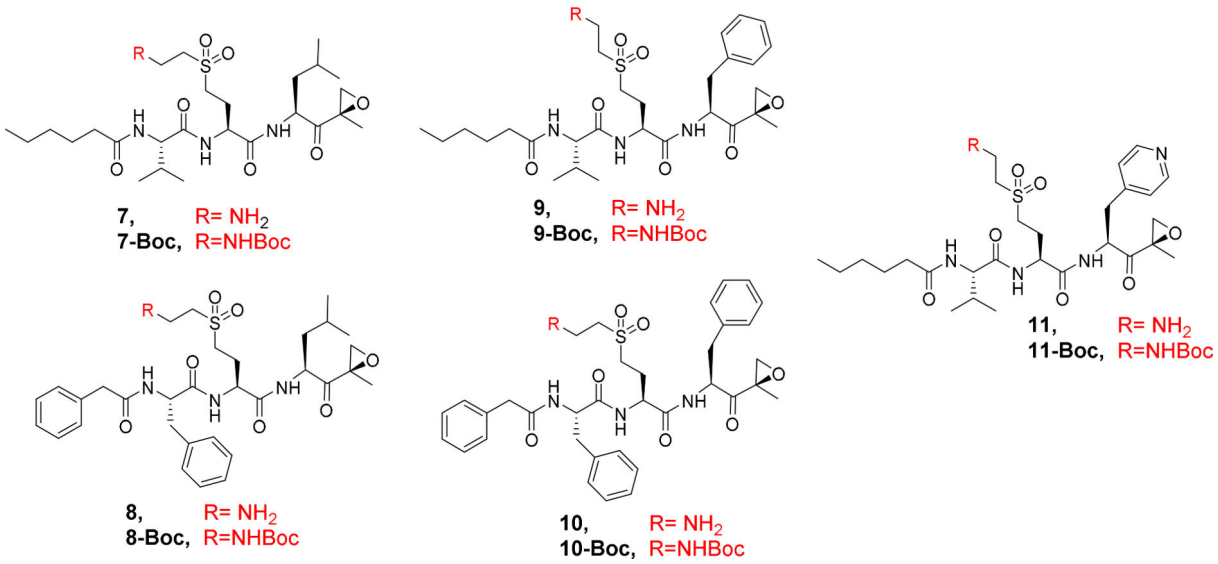

Figure 5.

Structure of carmaphycin B analogues **7–11** with the presence of an ethylamine handle for conjugation to the linker and antibody.

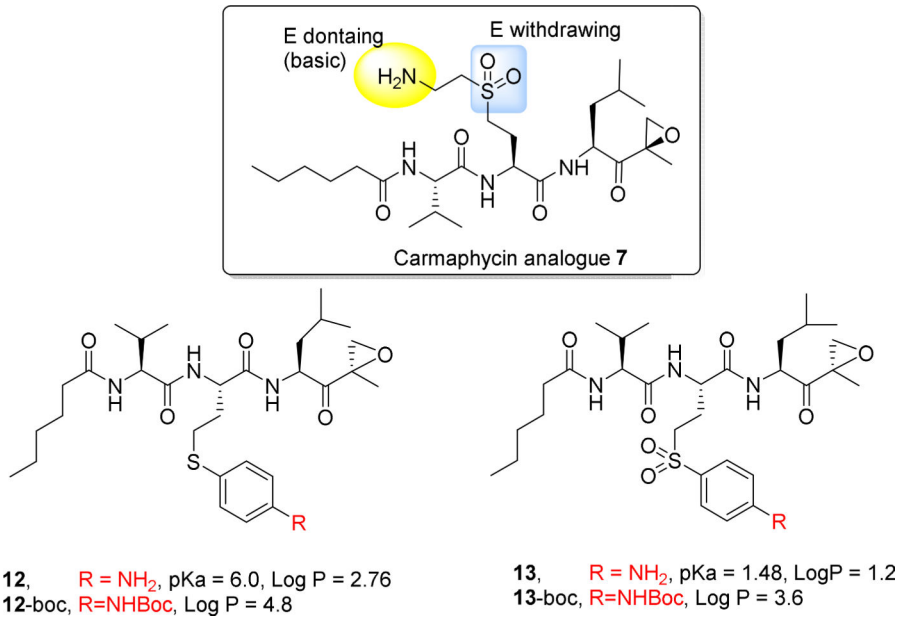

Figure 6.

Structures of non-basic amine containing analogues **12**, **13** and their Boc protected precursors (pKa and LogP were calculated using www.chemaxon.com).

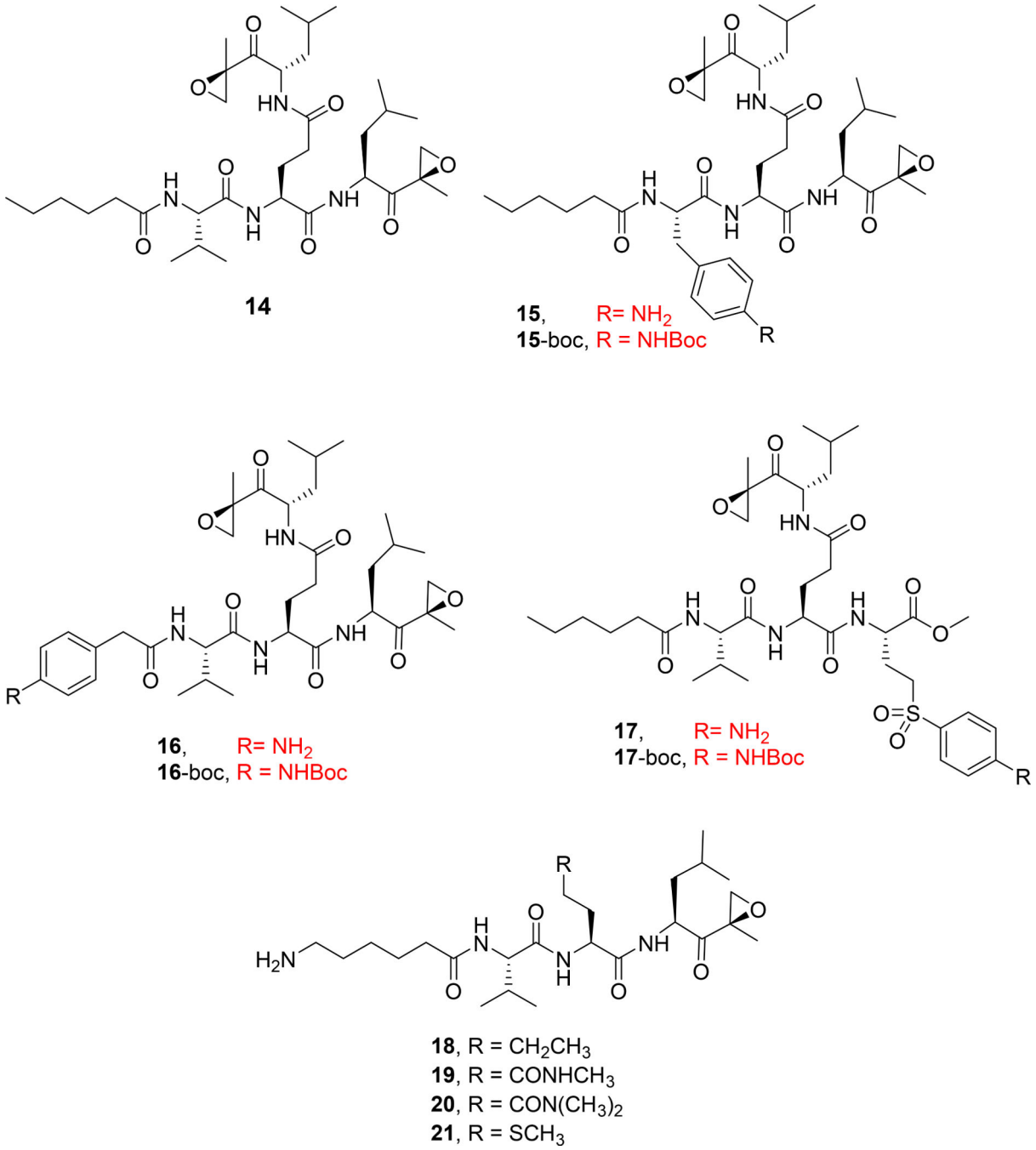

Figure 7.
Structures of analogues **14–21**.

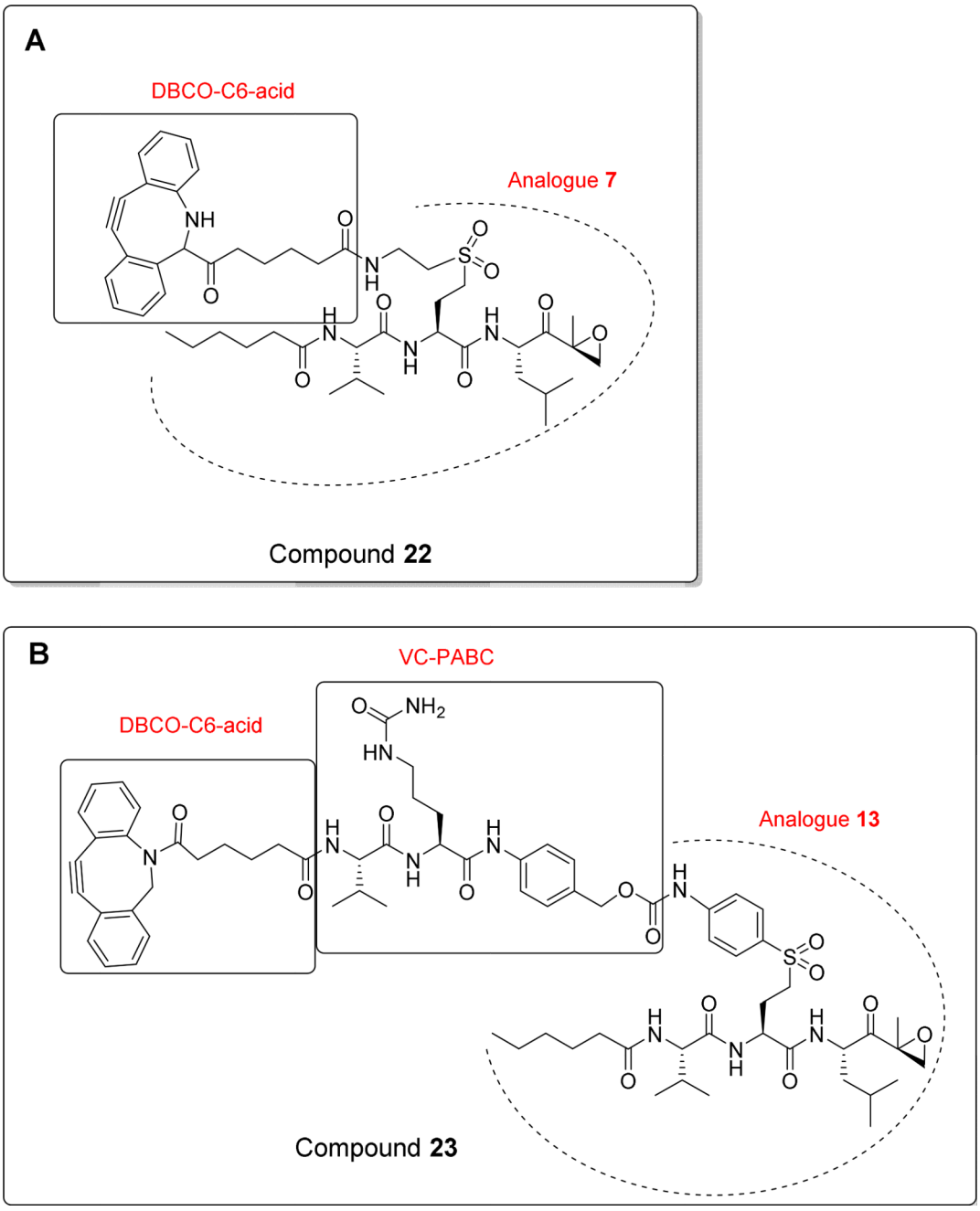

Figure 8.

Structures of ADC payload compounds: A) compound **22** in which analog **7** is attached to a non-cleavable linker, and B) compound **23** in which analog **13** is attached to a cleavable linker.

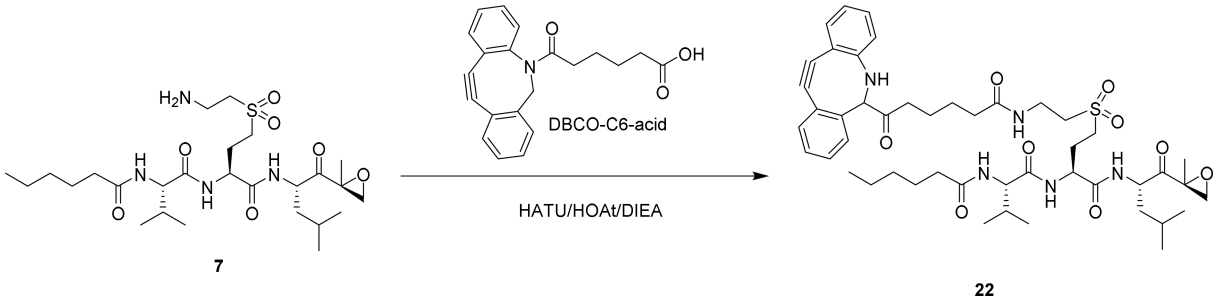

Figure 9.
Synthesis of non-cleavable linker payload, compound **22**.

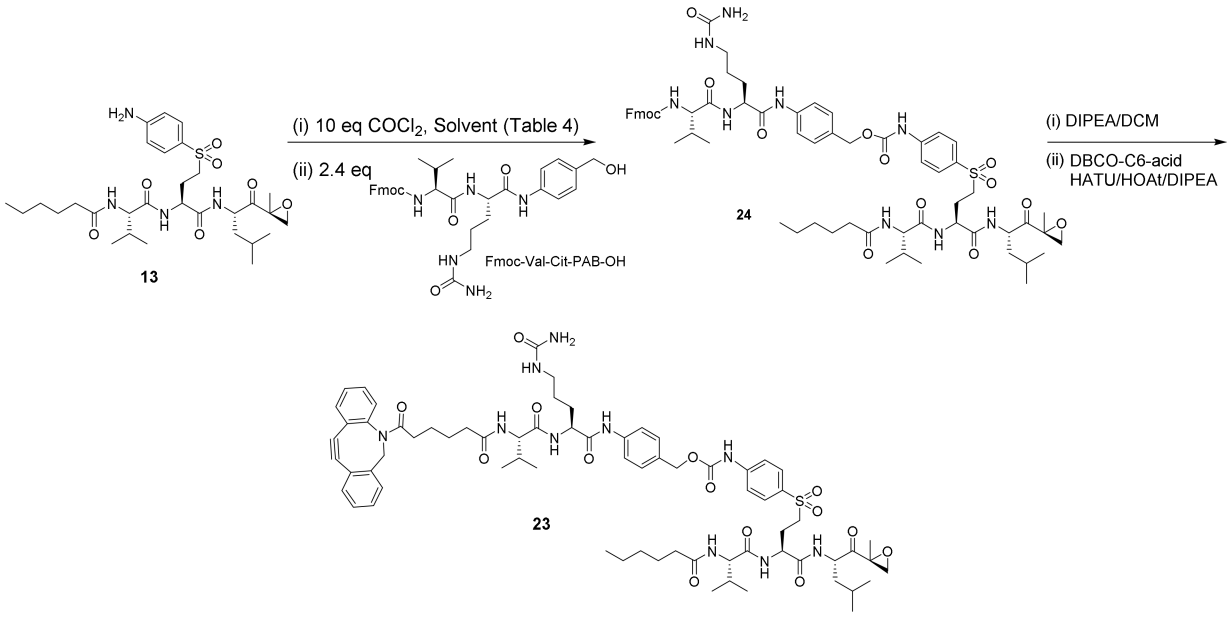

Figure10.
Synthesis of cleavable linker payload compound **23**

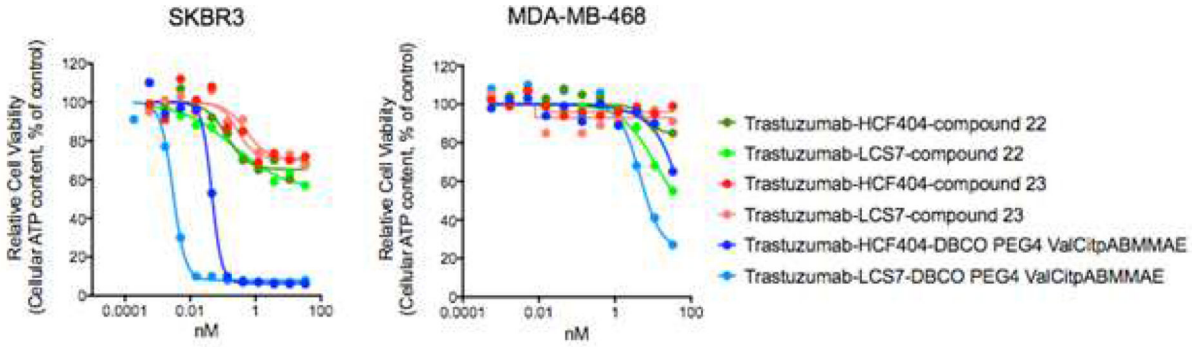

Figure 11.

Dose-response graphs for the ADC conjugates of analogues **22**, **23** and monomethyl auristatin E (**MMAE**) evaluated to SKBR3 and MDA-MB-468 cell lines.

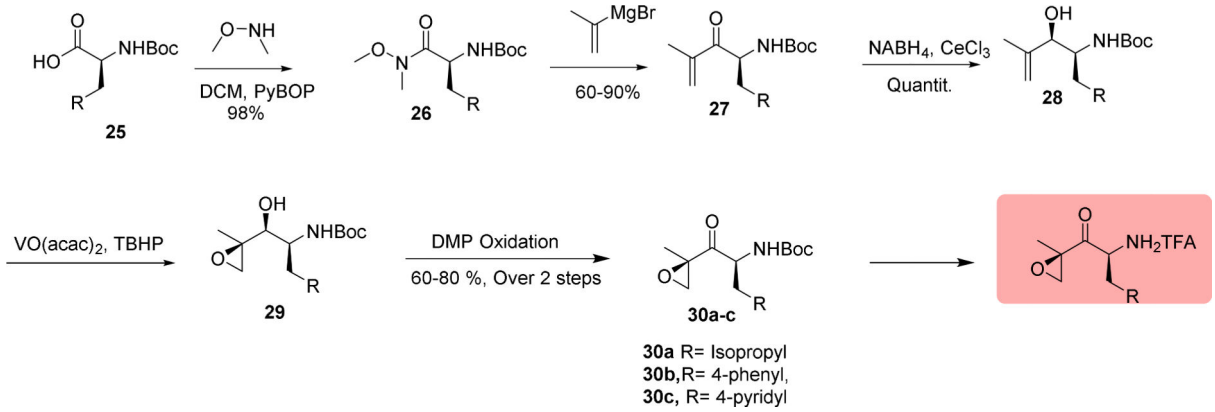

Scheme 1.

Generalized route for the synthesis of Boc-protected epoxyketones (**30a – 30c**).

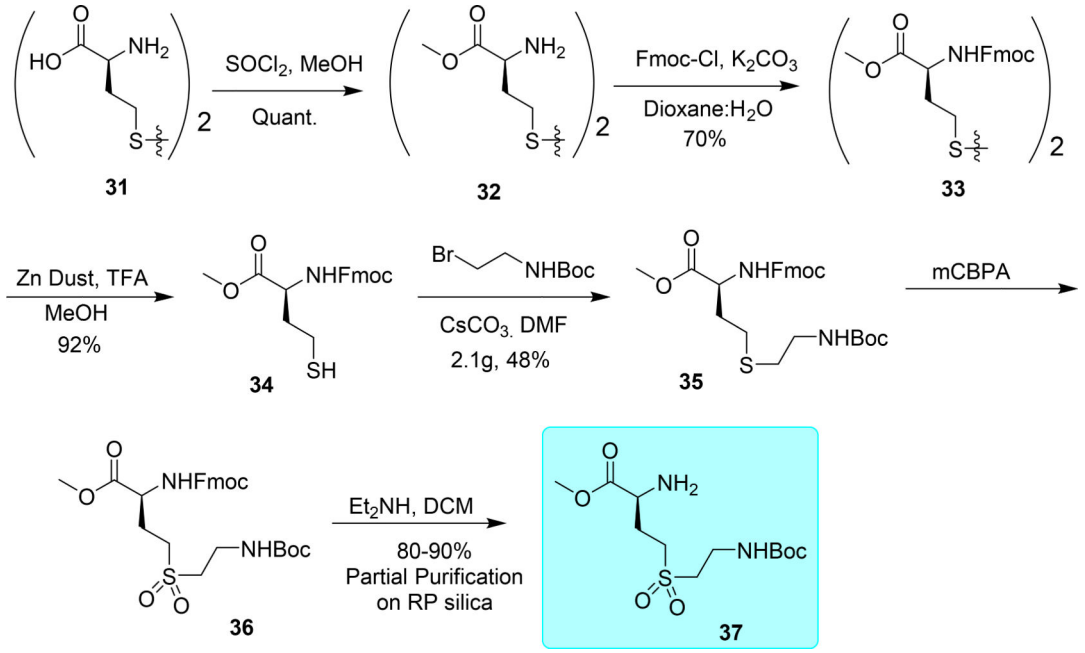

Scheme 2.

Synthesis of building block **37**.

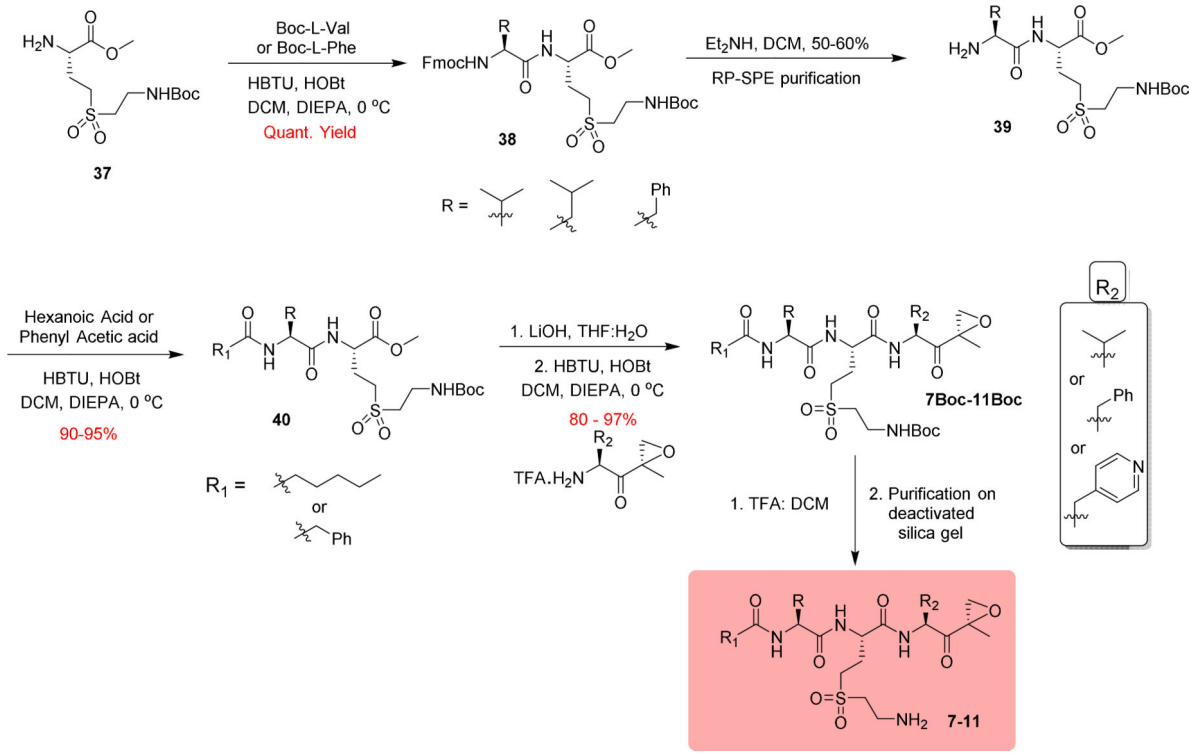

Scheme 3.

Synthesis of carmaphycin analogues **7–11**.

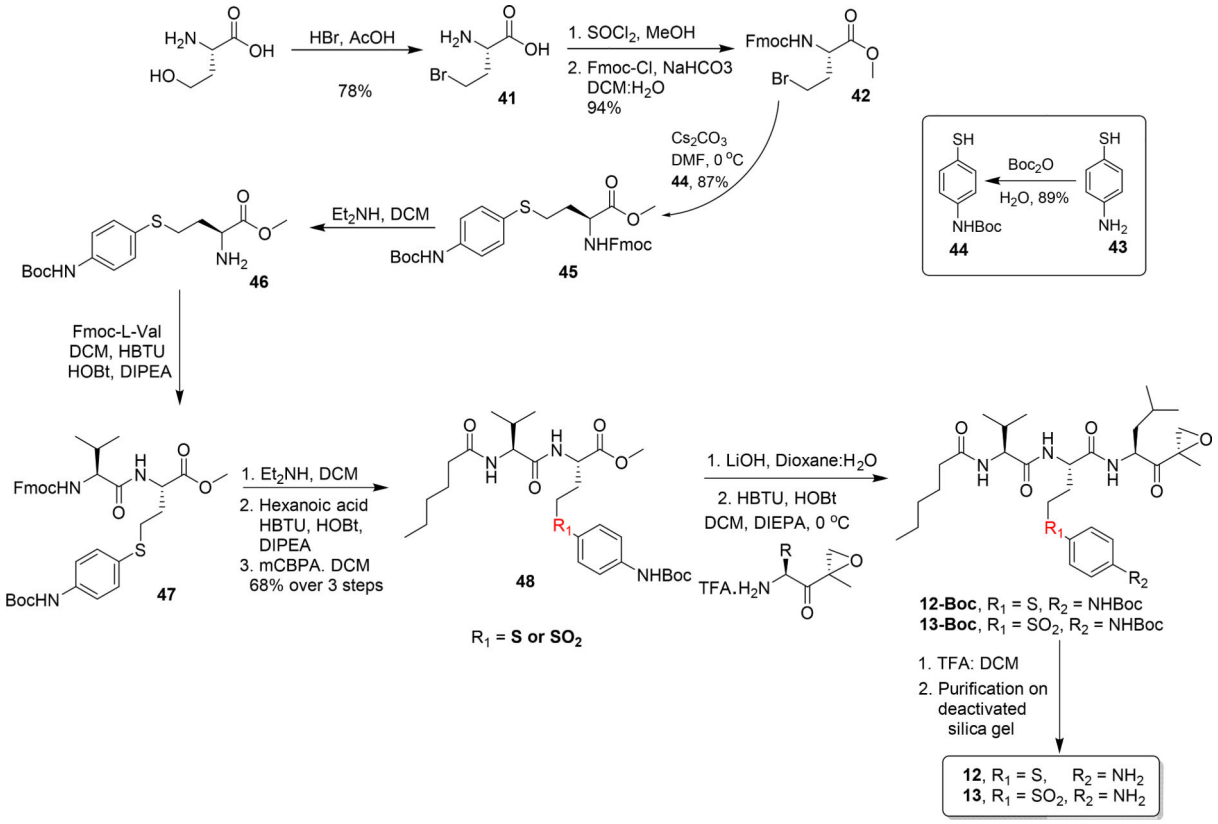

Scheme 4.

Synthesis of analogues **12** and **13**.

Table 1.

Evaluation of the cytotoxic properties of the designed analogues **6–14** in NCI-H460 and HCT116 cell line**s.**

Analogue #	NCI-H460 IC_{50} (nM)	HCT116 IC_{50} (nM)
6	860	ND
7	34	623.8
7-Boc	2.1±0.16	4.8±0.27
8	34.2	165.4
8-Boc	8.5±1.2	4.8±0.35
9	33.4	882.4
9-Boc	2.6±0.12	1.3±0.20
10	304.0	698.0
10-Boc	21.0±1.3	10.9±0.98
11	68.5	ND
11-Boc	30.2±2.1	ND
12	22	37.1
12-Boc	27	45.9
13	1.8±0.1	2.6±0.2
13-Boc	6.6±0.3	4.9±0.1
14	5.4±1.0	0.2±0.1

ND: Not Determined

Table 2.

Biological evaluation of analogues **15–21** in NCI-H460, HCT116, MDA-MB-468, and SKBR3 cell line**s.**

Analogue #	NCI-H460 IC_{50} (nM)	HCT116 IC_{50} (nM)	MDA-MB-468 IC_{50} (nM)	SKBR3 IC_{50} (nM)
15	29.8	53	30	21
15-Boc	52.6	132	140	39
16	25.3	45	33	25
16-Boc	6.8	9.2	7.8	6.6
17	>10000	5545	1745	2427
17-Boc	9109	7345	4421	4083
18	4650±21	8459±959	ND	ND
19	34±8.2	67	ND	ND
20	26±3.4	18	ND	ND
21	27±2.6	22	ND	ND

Table 3.

Inhibitory effects of compounds **7** and **13–17** on the three human 20S proteasome active sites.

Analogue	ChT-L activity (nM)	T-L activity (nM)	C-L activity (nM)
7	42.2 ± 5.4	ND	ND
7-Boc	14.2 ± 2.4	ND	ND
13	1.5 ± 0.2	14	540
14	1.9 ± 0.1	98.0	150
15	5.6	315	>1000
15-Boc	4.8	201	>1000
16	90 ± 13	71.5	>1000
16-Boc	100 ± 15	82	568
17	>1000	>1000	>1000

ND: Not determined

Table 4.

Optimization of reaction conditions to obtain product **24** (*yields determined by LCMS)

Rxn #	Solvent	Temperature	Time	Conditions	Yield *
1	THF	Reflux	O/N	Reflux in RB flask	<5%
2	THF+DCE	Reflux	O/N	Sealed tube	13%
3	Dioxane	Reflux	O/N	Reflux in RB flask	8%
4	Acetonitrile	Reflux	O/N	Reflux in RB flask	17%
5	Acetonitrile	Reflux	O/N	Sealed tube	23%
6	EA	Reflux	O/N	Sealed tube	12%
7	EA+DCE	Reflux	O/N	Sealed tube	17%
8	DMF	Reflux	O/N	Reflux in RB flask	<5%
9	Acetonitrile	110 °C	1 hr	Microwave	<5%
10	EA	110 °C	1 hr	Microwave	<5%

Table 5.

Biological evaluation of analogues **7-Boc**, **13**, **22** and **23** and their ADC conjugates in the SKBR3, MDA-MB-468 and MDA-MB-231 cell lines.

	Her2+ cell	**Her2- cell**		
	SKBR3 IC_{50} (nM)	**MDA-MB-468 IC_{50} (nM)**	**MDA-MB-231 IC_{50} (nM)**	**NCI-H460 IC_{50} (nM)**
7-Boc	12.0	19.0	1.3	2.1±0.16
13	0.430	9.6	0.140	1.8±0.1
MMAE	0.072	0.17	0.005	---
23	15.8	---	12.8	---
Trastuzumab-LCS7-**22**	0.21	12	---	> 100
Trastuzumab-HCF404-**22**	0.13	6.6*	---	> 100
Trastuzumab-LCS7-**23**	0.53	>100	---	> 100
Trastuzumab-HCF404-**23**	0.28	>100	10.0	> 100
Trastuzumab-LCS7-**MMAE**	0.003	4.6	---	---
Trastuzumab-HCF404-**MMAE**	0.046	>100	---	---